A genome-wide screen for genes affecting spontaneous direct-repeat recombination in *Saccharomyces cerevisiae*

Daniele Novarina[*], Ridhdhi Desai[†], Jessica A. Vaisica[†], Jiongwen Ou[†], Mohammed Bellaoui[†,1], Grant W. Brown[†,2] and Michael Chang[*,3]

[*]European Research Institute for the Biology of Ageing, University of Groningen, University Medical Center Groningen, 9713 AV Groningen, the Netherlands

[†]Department of Biochemistry and Donnelly Centre, University of Toronto, Toronto, ON M5S 3E1, Canada

[1]Current address: Genetics Unit, Faculty of Medicine and Pharmacy, University Mohammed Premier, Oujda, Morocco

[2]Co-corresponding author: Department of Biochemistry and Donnelly Centre, University of Toronto, 160 College Street, Toronto, ON M5S 3E1 Canada. E-mail: grant.brown@utoronto.ca

[3]Co-corresponding author: European Research Institute for the Biology of Ageing, University of Groningen, University Medical Center Groningen, Antonius Deusinglaan 1, 9713 AV Groningen, the Netherlands. E-mail: m.chang@umcg.nl

Running title: **Spontaneous recombination screen**

Keywords:

Homologous recombination

Direct repeat

Functional genomics

Saccharomyces cerevisiae

Genome stability

DNA damage

DNA repair

ABSTRACT

Homologous recombination is an important mechanism for genome integrity maintenance, and several homologous recombination genes are mutated in various cancers and cancer-prone syndromes. However, since in some cases homologous recombination can lead to mutagenic outcomes, this pathway must be tightly regulated, and mitotic hyper-recombination is a hallmark of genomic instability. We performed two screens in *Saccharomyces cerevisiae* for genes that, when deleted, cause hyper-recombination between direct repeats. One was performed with the classical patch and replica-plating method. The other was performed with a high-throughput replica-pinning technique that was designed to detect low-frequency events. This approach allowed us to validate the high-throughput replica-pinning methodology independently of the replicative aging context in which it was developed. Furthermore, by combining the two approaches, we were able to identify and validate 35 genes whose deletion causes elevated spontaneous direct-repeat recombination. Among these are mismatch repair genes, the Sgs1-Top3-Rmi1 complex, the RNase H2 complex, genes involved in the oxidative stress response, and a number of other DNA replication, repair and recombination genes. Since several of our hits are evolutionary conserved, and repeated elements constitute a significant fraction of mammalian genomes, our work might be relevant for understanding genome integrity maintenance in humans.

INTRODUCTION

Homologous recombination (HR) is an evolutionarily conserved pathway that can repair DNA lesions, including double-strand DNA breaks (DSBs), single-strand DNA (ssDNA) gaps, collapsed replication forks, and interstrand crosslinks, by using a homologous sequence as the repair template. HR is essential for the maintenance of genome integrity, and several HR genes are mutated in human diseases, especially cancers and cancer-prone syndromes (Krejci et al., 2012; Symington et al., 2014). HR is also required for meiosis (Hunter, 2015) and is important for proper telomere function (Claussin and Chang, 2015). The yeast *Saccharomyces cerevisiae* has been a key model organism for determining the mechanisms of eukaryotic recombination. Our current understanding of the HR molecular pathway comes mainly from the study of DSB repair. However, most mitotic HR events are likely not due to the repair of DSBs (Claussin et al., 2017), and can be triggered by diverse DNA structures and lesions, including DNA nicks, ssDNA gaps, arrested or collapsed replication forks, RNA-DNA hybrids and noncanonical secondary structures (Symington et al., 2014). An essential intermediate in recombination is ssDNA, which, in the case of a DSB, is generated by resection of the DSB ends by nucleases. Rad52 stimulates the loading of Rad51 onto ssDNA, which in turn mediates homologous pairing and strand invasion, with the help of Rad54, Rad55, and Rad57. After copying the homologous template, recombination intermediates are resolved with the help of nucleases and helicases, and the HR machinery is disassembled (Symington et al., 2014).

While HR is important for genome integrity, excessive or unregulated recombination in mitotic cells can be deleterious. Indeed, even though HR is generally considered an error-free DNA repair pathway, outcomes of HR can be mutagenic. For instance, single strand annealing (SSA) occurring between direct repeats results in the deletion of the intervening sequence

(Bhargava et al., 2016), while recombination between ectopic homolog sequences can lead to gross chromosomal rearrangements (Heyer, 2015). Mutations and chromosomal aberrations can be the outcome of recombination between slightly divergent DNA sequences, a process termed "homeologous recombination" (Spies and Fishel, 2015). Allelic recombination between homologous chromosomes can lead to loss of heterozygosity (LOH) (Aguilera and García-Muse, 2013). Finally, the copying of the homologous template occurs at lower fidelity than is typical for replicative DNA polymerases, resulting in mutagenesis (McVey et al., 2016). For these reasons, the HR process must be tightly controlled, and spontaneous hyper-recombination in mitotic cells is a hallmark of genomic instability (Aguilera and García-Muse, 2013; Heyer, 2015).

Pioneering mutagenesis-based screens led to the identification of hyper-recombination mutants (Aguilera and Klein, 1988; Keil and McWilliams, 1993). Subsequently, several systematic screens were performed with the yeast knockout (YKO) collection to identify genes whose deletion results in a spontaneous hyper-recombinant phenotype. In particular, Alvaro et al. screened an indirect phenotype, namely elevated spontaneous Rad52 focus formation in diploid cells, which led to the identification of hyper-recombinant as well as recombination-defective mutants (Alvaro et al., 2007). A second screen for elevated Rad52 foci in haploid cells identified additional candidate recombination genes (Styles et al., 2016), although the recombination rates of these were not assessed directly. A distinct screen of the YKO collection measured elevated spontaneous LOH events in diploid cells, which arise through recombination between homologous chromosomes or as a consequence of chromosome loss (Andersen et al., 2008). Here we describe two systematic genome-scale screens measuring spontaneous recombination in haploid cells, since the sister chromatid is generally a preferred template for mitotic recombination relative to the homologous chromosome, both in yeast and mammalian cells (Johnson and Jasin, 2000; Kadyk and Hartwell, 1992). We use a direct-repeat recombination

assay (Smith and Rothstein, 1999), because recombination between direct repeats can have a significant impact on the stability of mammalian genomes, where tandem and interspersed repeated elements, such as LINEs and SINEs, are very abundant (George and Alani, 2012; López-Flores and Garrido-Ramos, 2012).

Recombination rate screens were performed both with the classical patch and replica-plating method and with our recently developed high-throughput replica-pinning technique, which was designed for high-throughput screens involving low-frequency events (Novarina et al., 2020). High-throughput replica-pinning is based on the concept that, by robotically pinning an array of yeast strains many times in parallel, several independent colonies per strain can be analysed at the same time, giving a semi-quantitative estimate of the rate at which a specific low-frequency event occurs in each strain. We used both approaches to screen the YKO collection with the direct-repeat recombination assay. Bioinformatic analysis and direct comparison of the two screens confirmed the effectiveness of the high-throughput replica-pinning methodology. Together, we identified and validated 35 genes whose deletion results in elevated spontaneous direct-repeat recombination, many of which have homologs or functional counterparts in humans.

120 MATERIALS AND METHODS

121

122 **Yeast strains and growth conditions**

123 Standard yeast media and growth conditions were used (Sherman, 2002; Treco and Lundblad,
124 2001). All yeast strains used in this study are derivatives of the BY4741 genetic background
125 (Brachmann et al., 1998) and are listed in Supporting Information, Table S1.

126

127 **Patch and replica-plating screen**

128 To create a recombination assay strain compatible with Synthetic Genetic Array (SGA)
129 methodology (Kuzmin et al., 2016), the *leu2ΔEcoRI-URA3-leu2ΔBstEII* direct repeat
130 recombination reporter (Smith and Rothstein, 1999) was introduced into Y5518 by PCR of the
131 *LEU2* locus from W1479-11C, followed by transformation of Y5518 and selection on SD-ura.
132 Correct integration was confirmed by PCR, and the resulting strain was designated JOY90.
133 JOY90 was then crossed to the *MAT***a** yeast knockout (YKO) collection ((Giaever et al., 2002);
134 gift of C. Boone, University of Toronto), using SGA methodology (Kuzmin et al., 2016).
135 Following selection on SD-his-arginine-lysine-uracil+G418+ClonNat+canavanine+thialysine, the
136 resulting strains have the genotype *MAT***a** *xxx*Δ*::kanMX mfa1Δ::MFA1pr-HIS3*
137 *leu2*Δ*EcoRI::URA3-HOcs::leu2*Δ*BstEII his3*Δ*1 ura3*Δ*0 met15*Δ*0 lyp1*Δ *can1*Δ*::natMX*, where
138 *xxx*Δ*::kanMX* indicates the YKO gene deletion in each resulting strain.

139 Each YKO strain carrying the recombination reporter was streaked for single colonies on
140 SD-ura. Single colonies were then streaked in a 1 cm x 1 cm patch on YPD, incubated at 30°C
141 for 24 h, and then replica-plated to SD-leu to detect recombination events as papillae on the
142 patch. RDY9 (wild-type) and RDY13 (*elg1*Δ*::kanMX*; positive control) were included on each
143 plate. The papillae on SD-leu were scored by visual inspection relative to the control strains,

yielding 195 positives (Table S2). The 195 positives were tested in a fluctuation test of 5 independent cultures, and those with a recombination rate of at least $2x10^{-5}$ (approximately twofold greater than that of RDY9) were identified (43 strains; Table S2). Positives from the first fluctuation tests (except *slm3*Δ and *pex13*Δ, where rates could not be determined due to the large numbers of 'jackpot' cultures where all colonies had a recombination event) were assayed further, again with 5 cultures per fluctuation test. Thirty-three gene deletion mutants displayed a statistically supported increase in recombination rate (Table S2, Figure 1D), using a one-sided Student's t-test with a cutoff of p=0.05.

Fluctuation tests of spontaneous recombination rates

Fluctuation tests as designed by Luria and Delbrück (Luria and Delbrück, 1943) were performed by transferring entire single colonies from YPD plates to 4 ml of YPD liquid medium. Cultures were grown at 30°C to saturation. 100 µl of a 10^5-fold dilution were plated on a fully supplemented SD plate and 200 µl of a 10^2-fold dilution were plated on an SD-leu plate. Colonies were counted after incubation at 30°C for 3 days. The number of recombinant (leu+) colonies per 10^7 viable cells was calculated, and the median value was used to determine the recombination rate by the method of the median (Lea and Coulson, 1949).

High-throughput replica pinning screen

High-throughput manipulation of high-density yeast arrays was performed with the RoToR-HDA pinning robot (Singer Instruments). The *MAT***a** yeast deletion collection (EUROSCARF) was arrayed in 1536 format (each strain in quadruplicate). The *leu2ΔEcoRI-URA3-leu2ΔBstEII* marker to measure direct-repeat recombination (Smith and Rothstein, 1999) was introduced into the deletion collection through synthetic genetic array (SGA) methodology (Kuzmin et al., 2016)

using the JOY90 query strain. The procedure was performed twice in parallel to generate two sets of the yeast deletion collection containing the *leu2* direct-repeat recombination reporter. Each plate of each set was then pinned onto six YPD+G418 plates (48 replicates per strain in total), incubated for one day at 30° and then scanned with a flatbed scanner. Subsequently, each plate was pinned onto SD-leu solid medium and incubated for two days at 30° to select recombination events. Finally, all plates were re-pinned on SD-leu solid medium and incubated for one day at 30° before scanning. Colony area measurement was performed using the ImageJ software package (Schneider et al., 2012) and the ScreenMill Colony Measurement Engine plugin (Dittmar et al., 2010), to assess colony circularity and size in pixels. Colony data was filtered to exclude artifacts by requiring a colony circularity score greater than 0.8. Colonies with a pixel area greater than 50% of the mean pixel area were scored for strains pinned to YPD+G418. Following replica-pinning to SD-leu, colonies were scored if the pixel area was greater than 10% of the mean pixel area for the same strain on YPD+G418. For each deletion strain, the ratio of recombinants (colonies on SD-leu) to total colonies (colonies on YPD+G418) is the recombination frequency (Table S3). Strains where fewer than 10 colonies grew on YPD+G418 were removed from consideration, as were the 73 YKO collection strains carrying an additional *msh3* mutation (Lehner et al., 2007). The final filtered data is presented in Table S4.

Gene Ontology enrichment analysis and functional annotation

GO term analysis was performed using the GO term finder tool (http://go.princeton.edu/) using a P-value cutoff of 0.01 and applying Bonferroni correction, querying biological process enrichment for each gene set. GO term enrichment results were further processed with REViGO (Supek et al., 2011) using the “Medium (0.7)” term similarity filter and simRel score as the semantic similarity measure. Terms with a frequency greater than 15% in the REViGO output

were eliminated as too general. Gene lists used for the GO enrichment analyses are in Table 1, and the lists of enriched GO terms obtained are provided in Table S6. Human orthologues in Table 3 were identified using YeastMine (https://yeastmine.yeastgenome.org/yeastmine; accessed June 25, 2019). Protein-protein interactions were identified using GeneMania (https://genemania.org/; (Warde-Farley et al., 2010)), inputting the 35 validated hyper-rec genes, and selecting only physical interactions, zero resultant genes, and equal weighting by network. Network edges were reduced to a single width and nodes were annotated manually using gene ontology from the *Saccharomyces* Genome Database (https://www.yeastgenome.org). Network annotations were made with the Python implementation of Spatial Analysis of Functional Enrichment (SAFE) (Baryshnikova, 2016); https://github.com/baryshnikova-lab/safepy). The yeast genetic interaction similarity network and its functional domain annotations were obtained from (Costanzo et al., 2016). The genetic interaction scores for *YER188W*, *DFG16*, *VMA11*, and *ABZ2* were downloaded from the Cell Map (http://thecellmap.org/; accessed January 9, 2020),

Statistical analysis

Statistical analysis was performed in Excel or R (https://cran.r-project.org/).

Data availability

Strains are available upon request. A file containing supplemental tables is available at FigShare. Table S1 lists all the strains used in this study. Table S2 contains the fluctuation test data from the patch screen. Table S3 contains the raw high-throughput replica pinning screen data. Table S4 contains the filtered pinning screen data. Table S5 contains the fluctuation test data from the pinning screen. Table S6 contains the GO term enrichment data.

RESULTS

A genetic screen for elevated spontaneous direct-repeat recombination

The *leu2* direct-repeat recombination assay (Smith and Rothstein, 1999) can detect both intra-chromosomal and sister chromatid recombination events (Figure 1A). Two nonfunctional *leu2* heteroalleles are separated by a 5.3 kb region containing the *URA3* marker. Reconstitution of a functional *LEU2* allele can occur either via sister chromatid recombination (gene conversion), which maintains the *URA3* marker, or via intra-chromosomal SSA, with the concomitant deletion of the sequence between the direct repeats and subsequent loss of the *URA3* marker (Symington et al., 2014). Both recombination events can be selected on media lacking leucine. We used this assay to systematically screen the yeast knockout (YKO) collection for genes whose deletion results in hyper-recombination between direct repeats (Figure 1B). We introduced the *leu2* direct-repeat recombination reporter into the YKO collection via synthetic genetic array (SGA) technology (Kuzmin et al., 2016). Each of the ~4500 obtained strains was then patched on non-selective plates and replica-plated to plates lacking leucine to detect spontaneous recombination events as papillae on the replica-plated patches (Figure 1C). We included a wild-type control and a hyper-recombinant *elg1*Δ control (Bellaoui et al., 2003; Ben-Aroya et al., 2003) on every plate for reference. The recombination rates for 195 putative hyper-rec mutants identified by replica-plating (Table S2) were measured by a fluctuation test. Strains with a recombination rate greater than $2x10^{-5}$ (approximately twofold of the wild-type rate; 38 strains) were assayed in triplicate (or more). Thirty-three gene deletion mutant strains with a statistically supported increase in direct-repeat recombination rate relative to the wild-type control were identified (Figure 1D, Table S2, Table 1). The genes identified showed a high degree of enrichment for GO terms reflecting roles in DNA replication and repair (Figure 1E).

A high-throughput screen for altered spontaneous direct-repeat recombination

We recently developed a high-throughput replica-pinning method to detect low-frequency events, and validated the scheme in a genome-scale mutation frequency screen (Novarina et al., 2020). To complement the data obtained with the classical screening approach, and to test our new methodology independently of the replicative aging context in which it was developed, we applied it to detect changes in spontaneous direct-repeat recombination (Figure 2A). We again introduced the *leu2* direct-repeat recombination reporter (Figure 1A) into the YKO collection. The collection was then amplified by parallel high-throughput replica-pinning to yield 48 colonies per gene deletion strain. After one day of growth, all colonies were replica-pinned (twice, in series) to media lacking leucine to select for recombination events. Recombination frequencies (a proxy for the spontaneous recombination rate) were calculated for each strain of the collection (Figure 2B, Table S3, Table S4). As a reference, recombination frequencies for the wild type (46%) and for a recombination-deficient *rad54*Δ strain (21%) obtained in a pilot replica-pinning experiment of 3000 colonies are indicated. In the screen itself, where 48 colonies were assessed, the wild type (*his3*Δ*::kanMX*) had a recombination frequency of 56%. Notably, a group of strains from the YKO collection carry an additional mutation in the mismatch repair gene *MSH3* (Lehner et al., 2007). Given the elevated spontaneous recombination rates of several mismatch repair-deficient strains (Figure 1D), we suspected that these *msh3* strains would display increased recombination frequencies, independently of the identity of the intended gene deletion. Indeed, the distribution of recombination frequencies for *msh3* strains (median: 74%) is shifted toward higher values compared to the overall distribution of the YKO collection (median: 60%) (Figure 2B). The 73 *msh3* strains were excluded from further analysis.

263 To explore the overall quality of the high-throughput replica-pinning screen and to
264 determine a cutoff in an unbiased manner, we performed Cutoff Linked to Interaction Knowledge
265 (CLIK) analysis (Dittmar et al., 2013). The CLIK algorithm identified an enrichment of highly
266 interacting genes at the top and at the bottom of our gene list (ranked according to recombination
267 frequency), confirming the overall high quality of our screen, and indicating that we were able to
268 detect both hyper- and hypo-recombinogenic mutants (Figure 2C). The cutoff indicated by CLIK
269 corresponds to a recombination frequency of 87% for the hyper-recombination strains (75 genes;
270 Table 1), and of 33% for the recombination-deficient strains (122 genes; Table 2).
271
272 *Hyper-recombination genes.* We assessed the functions of the 75 hyper-recombination genes
273 identified by our high-throughput screen (Figure 2D). As with the genes identified in the patch
274 screen, the genes identified in the pinning screen were enriched for DNA replication and repair
275 functions. Most importantly, at the very top of our hyper-recombination gene list (with 96% to
276 100% recombination), 11 out of 13 genes were identified in the patch screen and validated by
277 fluctuation analysis (Table S2). We tested the two additional genes, *CSM1* and *NUP170*, by
278 fluctuation analysis, and found that both had a statistically supported increase in recombination
279 rate (Figure 2E and Table S5). Eighteen validated hyper-recombination genes from the patch
280 screen were not identified in the pinning screen, and so are false negatives. Although we have not
281 validated the weaker hits from the pinning screen (those with recombination frequencies between
282 87% and 96%), four genes in this range were validated as part of the patch screen (*APN1*, *RMI1*,
283 *YLR235C*, and *RNH201*), 9 caused elevated levels of Rad52 foci when deleted (*APN1*, *NFI1*,
284 *RMI1*, *POL32*, *RNH201*, *DDC1*, *HST3*, *MFT1*, and *YJR124C*) (Alvaro et al., 2007; Styles et al.,
285 2016), and 3 are annotated as 'mitotic recombination increased' (*RMI1*, *DDC1*, and *HST3*;

Saccharomyces Genome Database). Together these data suggest that additional bona fide hyper-recombination genes were identified in the pinning screen.

Hypo-recombination genes. By contrast to the replica-plating screen, the pinning screen detected mutants with reduced recombination frequency, with 122 genes identified (Table 2). The genes identified were functionally diverse, with no gene ontology (GO) processes enriched. Only 19 nonessential genes are annotated as having reduced recombination as either null or hypomorphic alleles in the *Saccharomyces* genome database (SGD; accessed January 11, 2020 via YeastMine). Of these, three genes (*RAD52*, *LRP1*, and *THP1*) were detected in the pinning screen. In addition, other members of the *RAD52* epistasis group important for effective homologous recombination (*RAD50*, *RAD54* and *RAD55*) displayed a recombination frequency lower than 33%, and *RAD51* was just above the cutoff (Table S3). Thus, our high-throughput replica-pinning approach detects mutants with very low recombination frequencies. More generally, this observation suggests that if the pinning procedure is properly calibrated, a high-throughput replica-pinning screen is able not only to detect mutants with increased rates of a specific low-frequency event (in this case direct-repeat recombination), but also mutants with reduced rates of the same low-frequency event.

Validated hyper-recombination genes identified in both screens. We compared the genes identified in the pinning screen with those identified in the patch screen, revealing 15 genes that were identified in both screens, a statistically supported enrichment (Figure 3A; hypergeometric p = 1.2×10^{-21}). Combining the results of the two screens, we validated 35 genes whose deletion results in elevated spontaneous direct-repeat recombination (Table 3). Analysis of the group of 35 hyper-rec genes revealed 68 pairwise protein-protein interactions (Figure 3B), with many cases

where several (if not all) members of the particular protein complex were identified. We found that 29 of the hyper-rec genes had at least one human orthologue (Table 3), indicating a high degree of conservation across the 35 validated genes. To assess the functional properties of the 35 gene hyper-rec set, we applied spatial analysis of functional enrichment (SAFE) (Baryshnikova, 2016) to determine if any regions of the functional genetic interaction similarity yeast cell map (Costanzo et al., 2016) are over-represented for the hyper-rec gene set (Figure 3C). We found a statistically supported over-representation of the hyper-rec genes in the DNA replication and repair neighbourhood of the genetic interaction cell map, highlighting the importance of accurate DNA synthesis in suppressing recombination. Finally, we compared the validated hyper-rec genes to relevant functional genomic instability datasets (*Saccharomyces* Genome Database annotation, (Alvaro et al., 2007; Hendry et al., 2015; Stirling et al., 2011; Styles et al., 2016); Figure 3D). Eight of our hyper-rec genes (*HTA2*, *MSH6*, *YER188W*, *ABZ2*, *PMS1*, *MSH2*, *DFG16*, and *VMA11*) were not identified in these datasets, indicating that our screens identified uncharacterized recombination genes. *HTA2*, *MSH6*, *PMS1*, *MSH2* have recombination phenotypes reported (see Discussion). Thus, we identify four genes without a characterized role in preventing recombination: *YER188W*, *ABZ2*, *DFG16*, and *VMA11*.

To infer gene function for the four genes lacking a characterized role in suppressing recombination, we again applied SAFE analysis (Baryshnikova, 2016) to annotate the functional genetic interaction similarity yeast cell map (Costanzo et al., 2016) to identify any regions that are enriched for genetic interactions with each of the four genes (Figure 4). Of particular interest, the mitochondrial functional neighbourhood is enriched for negative genetic interactions with *YER188W* (Figure 4), suggesting that deletion of *YER188W* confers sensitivity to mitochondrial dysfunction. Analysis of *DFG16* revealed enrichments for positive interactions in the RIM

signaling neighbourhood, which is expected (Barwell et al., 2005), but also for negative interactions in the DNA replication region of the map (Figure 4), indicating that *DFG16* is important for fitness when DNA replication is compromised. Analysis of *VMA11* revealed enrichment in the vesicle trafficking neighbourhood, typical of vacuolar ATPase subunit genes, and analysis of *ABZ2* revealed little (Figure 4). We conclude that functional analysis suggests mechanisms by which loss of *YER188W* (oxidative stress) or *DFG16* (genome integrity) results in hyper-recombination.

DISCUSSION

Here we briefly discuss the functions of the genes and complexes identified in the screens and subsequently validated by fluctuation analysis.

Mismatch repair: *MLH1*, *MSH2*, *MSH6* and *PMS1* are evolutionary conserved genes involved in mismatch repair (MMR), a pathway that detects and corrects nucleotide mismatches in double-strand DNA (Spies and Fishel, 2015). An anti-recombinogenic role for these four MMR genes in yeast has been previously described: specifically, MMR proteins are important to prevent homeologous recombination and SSA between slightly divergent sequences, via mismatch recognition and heteroduplex rejection (Datta et al., 1996; Nicholson et al., 2000; Spies and Fishel, 2015; Sugawara et al., 2004). The role for MMR in preventing homeologous recombination is conserved also in mammalian cells (de Wind et al., 1995; Elliott and Jasin, 2001; Spies and Fishel, 2015). It is worth noting that the presence of sequence differences between the two *leu2* alleles in the *leu2* direct-repeat assay is essential to genetically detect recombination events. Therefore, it is reasonable that this assay should detect genes involved in suppressing homeologous recombination.

Sgs1-Top3-Rmi1 complex: The evolutionary conserved helicase-topoisomerase complex Sgs1-Top3-Rmi1 is involved in DSB resection and in dissolution of recombination intermediates (Symington et al., 2014). Consistent with previous observations (Chang et al., 2005), our screen identified all three members of the complex, together with *YLR235C*, a dubious ORF that overlaps the *TOP3* gene. The Sgs1-Top3-Rmi1 complex dissolves double Holliday junction structures to prevent crossover formation (Cejka et al., 2010). The same role has been reported for BLM helicase, the human Sgs1 homolog mutated in the genome stability disorder Bloom syndrome (Wu et al., 2006; Yang et al., 2010). Furthermore, several genetic studies indicate that the anti-recombinogenic activity of Sgs1-Top3-Rmi1 cooperates with MMR proteins in heteroduplex rejection to prevent homeologous recombination (Chakraborty et al., 2016; Goldfarb and Alani, 2005; Myung et al., 2001; Spell and Jinks-Robertson, 2004; Sugawara et al., 2004).

MGS1: In our screen we also identified *MGS1*, the homolog of the WRN-interacting protein WRNIP1. Mgs1 displays DNA-dependent ATPase and DNA strand annealing activities. Deletion of *MGS1* causes hyper-recombination, including elevated direct-repeat recombination (Hishida et al., 2001). It seems that Mgs1 promotes faithful DNA replication by regulating Polδ, and promoting replication fork restart after stalling (Branzei et al., 2002; Saugar et al., 2012). The absence of Mgs1 could result in increased replication fork collapse, leading to the formation of recombinogenic DSBs (Branzei et al., 2002). Similar roles have been suggested for WRNIP1 in mammalian cells (Leuzzi et al., 2016; Tsurimoto et al., 2005).

RNase H2 complex: *RNH201* encodes the evolutionary conserved catalytic subunit of RNase H2, while the two non-catalytic subunits are encoded by *RNH202* and *RNH203* genes. This enzyme

cleaves the RNA moiety in RNA-DNA hybrids originating from Okazaki fragments, co-transcriptional R-loops, and ribonucleotide incorporation by replicative polymerases (Cerritelli and Crouch, 2009). Deletion of any of the three subunits in yeast inactivates the whole complex. Human RNase H2 genes are mutated in Aicardi-Goutières syndrome, a severe neurological disorder (Crow et al., 2006). Inactivation of yeast RNase H2 causes elevated LOH, ectopic recombination and direct-repeat recombination (Conover et al., 2015; Potenski et al., 2014), mostly dependent on Top1 activity. What is the recombinogenic intermediate accumulated in the absence of RNase H2? It has been suggested that Top1-dependent cleavage at the ribonucleotide site creates a nick that can be further converted into a recombinogenic DSB (Potenski et al., 2014). Recent genetic studies indicate that, while in the case of LOH events hyper-recombination is caused by Top1-dependent processing of single ribonucleotides incorporated by leading strand polymerases and/or by accumulation of recombinogenic R-loops (Conover et al., 2015; Cornelio et al., 2017; Keskin et al., 2014; O'Connell et al., 2015), elevated direct-repeat recombination results instead from Top1-dependent cleavage of stretches of ribonucleotides, resulting from defective R-loop removal or Okazaki fragment processing in the absence of RNase H2 (Epshtein et al., 2016). In line with this model, we also detected elevated direct-repeat recombination rate in the absence of the Thp2 member of the THO complex, which functions at the interface between transcription and mRNA export to prevent R-loop accumulation (Chavez et al., 2000; Huertas and Aguilera, 2003), *DST1*, which encodes a transcription elongation factor and is anti-recombinogenic (Owiti et al., 2017), and the flap endonuclease encoded by *RAD27*, which is involved in Okazaki fragment processing (Balakrishnan and Bambara, 2013) (Table 3). Furthermore, deletion of the dubious ORF *YDL162C*, also identified in our screen, likely affects the expression level of neighbouring *CDC9*, an essential gene encoding DNA Ligase I, involved in Okazaki fragment processing and ligation after ribonucleotide removal from DNA. Together,

406 available data suggest that different modes leading to accumulation of RNA-DNA hybrids or
407 unprocessed Okazaki fragments result in hyper-recombination.
408
409 ***Fork protection complex:*** Tof1 and Csm3 (Timeless and Tipin in human cells) form the fork
410 protection complex (FPC), involved in stabilization of replication forks, maintenance of sister
411 chromatid cohesion and DNA replication checkpoint signaling (Bando et al., 2009; Chou and
412 Elledge, 2006; Katou et al., 2003; Leman et al., 2010; Mayer et al., 2004; Mohanty et al., 2006;
413 Noguchi et al., 2004, 2003; Xu et al., 2004). Recently, Tof1 and Csm3 were implicated in
414 restricting fork rotation genome-wide during replication; they perform this role independently of
415 their interacting partner Mrc1, which we did not identify in our screen (Schalbetter et al., 2015).
416 In the absence of Tof1 or Csm3, excessive fork rotation can cause spontaneous DNA damage, in
417 the form of recombinogenic ssDNA and DSBs (Chou and Elledge, 2006; Schalbetter et al., 2015;
418 Sommariva et al., 2005; Urtishak et al., 2009). Indeed, depletion of Tof1 and Csm3 orthologues
419 results in accumulation of recombination intermediates in fission yeast and mouse cells (Noguchi
420 et al., 2004, 2003; Sommariva et al., 2005; Urtishak et al., 2009).
421
422 ***RRM3:*** The *RRM3* gene, encoding a 5′ to 3′ DNA helicase, was initially identified because its
423 absence causes hyper-recombination between endogenous tandem-repeated sequences (such as
424 the rDNA locus and the *CUP1* genes) (Keil and McWilliams, 1993). The Rrm3 helicase travels
425 with the replication fork and facilitates replication through genomic sites containing protein-DNA
426 complexes that, in its absence, cause replication fork stalling and breakage. Such Rrm3-
427 dependent sites include the rDNA, telomeres, tRNA genes, inactive replication origins,
428 centromeres, and the silent mating-type loci (Azvolinsky et al., 2006; Ivessa et al., 2003, 2000;

Schmidt and Kolodner, 2004; Torres et al., 2004). Intriguingly, a tRNA gene is located about 350 bp upstream the chromosomal location of the *leu2* direct-repeat recombination marker. Increased replication fork pausing in the absence of Rrm3 could cause recombinogenic DSBs, explaining the elevated direct-repeat recombination we observe in the *rrm3*Δ strain.

Oxidative stress response genes: *YAP1* and *SKN7* encode two transcription factors important for the activation of the cellular response to oxidative stress (Morano et al., 2012). The glutathione peroxidase encoded by *HYR1* has a major role in activating Yap1 in response to oxidative stress (Delaunay et al., 2002). *TSA1* is a Yap1 and Skn7 target and encodes a peroxiredoxin that scavenges endogenous hydrogen peroxide (Wong et al., 2004). Deletion of *TSA1* causes hyper-recombination between inverted repeats (Huang and Kolodner, 2005), and oxidative stress response genes (including *TSA1*, *SKN7* and *YAP1*) are synthetic sick or lethal with HR mutants (Pan et al., 2006; Yi et al., 2016). A likely explanation for the elevated direct-repeat recombination we measured in strains defective for the oxidative stress response, therefore, is that oxidative DNA damage generates replication blocking lesions and/or replication-associated DSBs, both of which are processed by the HR pathway (Huang and Kolodner, 2005). An alternative explanation could be that extensive oxidative DNA damage results in the saturation of the mismatch-binding step of MMR, compromising MMR-dependent heteroduplex rejection, resulting in increased homeologous recombination (Hum and Jinks-Robertson, 2018; Spies and Fishel, 2015).

Other DNA Repair genes: *APN1* encodes the main apurinic/apyrimidinic (AP) endonuclease involved in yeast base excision repair (BER). Removal of endogenous alkylating damage can generate abasic sites, which are mostly processed by Apn1 (Boiteux and Guillet, 2004; Popoff et

al., 1990; Xiao and Samson, 1993). In the absence of *APN1*, abasic sites accumulate, which can hamper DNA replication. The recombination pathway is involved in the repair and/or bypass of these abasic sites, as suggested by the genetic interactions between the BER and the HR pathways (Boiteux and Guillet, 2004; Swanson et al., 1999; Vance and Wilson, 2001). The *APN1* gene is adjacent to *RAD27*, and therefore it is also possible that the hyper-recombination phenotype of *apn1*Δ is due to a "neighbouring-gene effect" on *RAD27*, as was reported in the case of telomere length alteration (Ben-Shitrit et al., 2012).

HTA2, which encodes one copy of histone H2A, is of course important for appropriate nucleosome assembly. Reducing histone levels by deleting one H3-H4 gene pair or by partial depletion of H4 increases recombination (Clemente-Ruiz and Prado, 2009; Liang et al., 2012; Prado and Aguilera, 2005), and it is likely that reducing *HTA2* gene dosage also does so. Since histone depletion results in diverse chromatin defects, the exact mechanisms by which recombination is induced are elusive.

RAD4 encodes a key factor of nucleotide excision repair (NER), and is involved in direct recognition and binding of DNA damage (Prakash and Prakash, 2000), while *RAD6* is a key gene controlling the post replication repair (PRR) DNA damage tolerance pathway (Ulrich, 2005). Genetic studies suggest that BER, NER, PRR and HR can redundantly process spontaneous DNA lesions, and inactivation of one pathway shifts the burden on the others. This mechanism could explain why deletion of *RAD4* or *RAD6* causes a modest increase in spontaneous direct-repeat recombination (Swanson et al., 1999).

CSM1 encodes a nucleolar protein that serves as a kinetochore organizer to promote chromosome segregation in meiosis, and is involved in localization and silencing of rDNA and telomeres in mitotic cells (Poon and Mekhail, 2011). Interestingly, Csm1 is important to inhibit homologous recombination at the rDNA locus and other repeated sequences (Burrack et al.,

2013; Huang et al., 2006; Mekhail et al., 2008). The nuclear pore complex has an intimate connection to recombination, in that some DSBs move to and are likely repaired at the NPC (Freudenreich and Su, 2016). The NPC gene *NUP170* has not been directly implicated in DSB repair, but is important for chromosome segregation (Kerscher et al., 2001).

The unknowns (YER188W, ABZ2, DFG16, and VMA11): Unexpectedly, the top hyper-rec gene identified in our screen is *VMA11*, which encodes a subunit of the evolutionarily conserved vacuolar H^+-ATPase (V-ATPase), important for vacuole acidification and cellular pH regulation (Hirata et al., 1997; Kane, 2006; Umemoto et al., 1991). *VMA11* involvement in genome maintenance is suggested by the sensitivity of a *vma11*Δ strain to several genotoxic agents, namely doxorubicin, ionizing radiation, cisplatin and oxidative stress (Thorpe et al., 2004; Xia et al., 2007). V-ATPase defects in yeast result in endogenous oxidative stress and defective Fe/S cluster biogenesis as a consequence of mitochondrial depolarization (Hughes and Gottschling, 2012; Milgrom et al., 2007; Veatch et al., 2009). Of note, several DNA replication and repair factors are Fe/S cluster proteins (Veatch et al., 2009; Zhang, 2014). Therefore, the hyper-recombination phenotype of *vma11*Δ could be due to increased spontaneous DNA damage, caused by elevated endogenous oxidative stress and/or by defective DNA replication and repair as a consequence of compromised Fe/S cluster biogenesis. However, *VMA11* was not detected in screens for increased Rad52 foci (Alvaro et al., 2007; Styles et al., 2016), or in a screen for increased DNA damage checkpoint activation (Hendry et al., 2015), suggesting that spontaneous DNA damage might not accumulate to high levels in *vma11*Δ.

ABZ2 encodes an enzyme involved in folate biosynthesis (Botet et al., 2007). Folate deficiency and the resulting compromise of nucleotide synthesis could promote recombination, although yeast culture media are rich in folate, and the *ABZ2* genetic interaction profile reveals

no similarity to nucleotide biosynthesis genes (Usaj et al., 2017). *DFG16* encodes a predicted transmembrane protein involved in pH sensing (Barwell et al., 2005). Interestingly, SAFE analysis indicates a role for *DFG16* in DNA replication and/or DNA repair, in addition to the expected role in pH signaling. There is currently little insight into the function of *YER188W*. SAFE analysis indicates a possible role in mitochondrial function, however a protein product of *YER188W* has not been detected to date in either mass spectrometry or GFP fusion protein analyses (Breker et al., 2014; Ho et al., 2018; Huh et al., 2003).

ACKNOWLEDGMENTS

We thank Anastasia Baryshnikova for advice and assistance with the SAFE analysis. This work was supported by grants from the Netherlands Organisation for Scientific Research (Vidi grant 864.12.002 to MC) and the Canadian Institutes of Health Research (MOP-79368 and FDN-159913 to GWB).

LITERATURE CITED

Aguilera, A., García-Muse, T., 2013. Causes of genome instability. Annu. Rev. Genet. 47, 1–32. https://doi.org/10.1146/annurev-genet-111212-133232

Aguilera, A., Klein, H.L., 1988. Genetic control of intrachromosomal recombination in *Saccharomyces cerevisiae*. I. Isolation and genetic characterization of hyper-recombination mutations. Genetics 119, 779–790.

Alvaro, D., Lisby, M., Rothstein, R., 2007. Genome-wide analysis of Rad52 foci reveals diverse mechanisms impacting recombination. PLoS Genet. 3, 2439–2449. https://doi.org/10.1371/journal.pgen.0030228

Andersen, M.P., Nelson, Z.W., Hetrick, E.D., Gottschling, D.E., 2008. A genetic screen for increased loss of heterozygosity in *Saccharomyces cerevisiae*. Genetics 179, 1179–1195. https://doi.org/10.1534/genetics.108.089250

Azvolinsky, A., Dunaway, S., Torres, J.Z., Bessler, J.B., Zakian, V.A., 2006. The *S. cerevisiae* Rrm3p DNA helicase moves with the replication fork and affects replication of all yeast chromosomes. Genes Dev. 20, 3104–3116. https://doi.org/10.1101/gad.1478906

Balakrishnan, L., Bambara, R.A., 2013. Flap Endonuclease 1. Annu. Rev. Biochem. 82, 119–138. https://doi.org/10.1146/annurev-biochem-072511-122603

Bando, M., Katou, Y., Komata, M., Tanaka, H., Itoh, T., Sutani, T., Shirahige, K., 2009. Csm3, Tof1, and Mrc1 form a heterotrimeric mediator complex that associates with DNA replication forks. J. Biol. Chem. 284, 34355–34365. https://doi.org/10.1074/jbc.M109.065730

Barwell, K.J., Boysen, J.H., Xu, W., Mitchell, A.P., 2005. Relationship of *DFG16* to the Rim101p pH response pathway in *Saccharomyces cerevisiae* and *Candida albicans*. Eukaryot. Cell 4, 890–899. https://doi.org/10.1128/ec.4.5.890-899.2005

Baryshnikova, A., 2018. Spatial analysis of functional enrichment (SAFE) in large biological networks. Methods Mol. Biol. 1819, 249–268. https://doi.org/10.1007/978-1-4939-8618-7_12

Baryshnikova, A., 2016. Systematic functional annotation and visualization of biological networks. Cell Syst. 2, 412–421. https://doi.org/10.1016/j.cels.2016.04.014

Bellaoui, M., Chang, M., Ou, J., Xu, H., Boone, C., Brown, G.W., 2003. Elg1 forms an alternative RFC complex important for DNA replication and genome integrity. EMBO J. 22, 4304–4313. https://doi.org/10.1093/emboj/cdg406

Ben-Aroya, S., Koren, A., Liefshitz, B., Steinlauf, R., Kupiec, M., 2003. *ELG1*, a yeast gene required for genome stability, forms a complex related to replication factor C. Proc. Natl. Acad. Sci. U. S. A. 100, 9906–9911. https://doi.org/10.1073/pnas.1633757100

Ben-Shitrit, T., Yosef, N., Shemesh, K., Sharan, R., Ruppin, E., Kupiec, M., 2012. Systematic identification of gene annotation errors in the widely used yeast mutation collections. Nat.

553 Methods 9, 373–378. https://doi.org/10.1038/nmeth.1890

554 Bhargava, R., Onyango, D.O., Stark, J.M., 2016. Regulation of single-strand annealing and its
555 role in genome maintenance. Trends Genet. 32, 566–575.
556 https://doi.org/10.1016/j.tig.2016.06.007

557 Boiteux, S., Guillet, M., 2004. Abasic sites in DNA: Repair and biological consequences in
558 *Saccharomyces cerevisiae*. DNA Repair (Amst). 3, 1–12.
559 https://doi.org/10.1016/j.dnarep.2003.10.002

560 Botet, J., Mateos, L., Revuelta, J.L., Santos, M.A., 2007. A chemogenomic screening of
561 sulfanilamide-hypersensitive *Saccharomyces cerevisiae* mutants uncovers *ABZ2*, the gene
562 encoding a fungal aminodeoxychorismate lyase. Eukaryot. Cell 6, 2102–2111.
563 https://doi.org/10.1128/ec.00266-07

564 Brachmann, C.B., Davies, A., Cost, G.J., Caputo, E., Li, J., Hieter, P., Boeke, J.D., 1998.
565 Designer deletion strains derived from *Saccharomyces cerevisiae* S288C: a useful set of
566 strains and plasmids for PCR-mediated gene disruption and other applications. Yeast 14,
567 115–132. https://doi.org/10.1002/(SICI)1097-0061(19980130)14:2<115::AID-
568 YEA204>3.0.CO;2-2

569 Branzei, D., Seki, M., Onoda, F., Enomoto, T., 2002. The product of *Saccharomyces cerevisiae*
570 *WHIP*/*MGS1*, a gene related to replication factor C genes, interacts functionally with DNA
571 polymerase δ. Mol. Genet. Genomics 268, 371–386. https://doi.org/10.1007/s00438-002-
572 0757-3

573 Breker, M., Gymrek, M., Moldavski, O., Schuldiner, M., 2014. LoQAtE - Localization and
574 Quantitation ATlas of the yeast proteomE. A new tool for multiparametric dissection of
575 single-protein behavior in response to biological perturbations in yeast. Nucleic Acids Res.
576 42, D726–D730. https://doi.org/10.1093/nar/gkt933

577 Burrack, L.S., Applen Clancey, S.E., Chacon, J.M., Gardner, M.K., Berman, J., 2013. Monopolin
578 recruits condensin to organize centromere DNA and repetitive DNA sequences. Mol. Biol.
579 Cell. https://doi.org/10.1091/mbc.e13-05-0229

580 Cejka, P., Plank, J.L., Bachrati, C.Z., Hickson, I.D., Kowalczykowski, S.C., 2010. Rmi1
581 stimulates decatenation of double Holliday junctions during dissolution by Sgs1-Top3. Nat.
582 Struct. Mol. Biol. 17, 1377–1382. https://doi.org/10.1038/nsmb.1919

583 Cerritelli, S.M., Crouch, R.J., 2009. Ribonuclease H: the enzymes in eukaryotes. FEBS J. 276,
584 1494–1505. https://doi.org/10.1111/j.1742-4658.2009.06908.x

585 Chakraborty, U., George, C.M., Lyndaker, A.M., Alani, E., 2016. A delicate balance between
586 repair and replication factors regulates recombination between divergent DNA sequences in
587 *Saccharomyces cerevisiae*. Genetics 202, 525–540.
588 https://doi.org/10.1534/genetics.115.184093

589 Chang, M., Bellaoui, M., Zhang, C., Desai, R., Morozov, P., Delgado-Cruzata, L., Rothstein, R.,
590 Freyer, G.A., Boone, C., Brown, G.W., 2005. *RMI1*/*NCE4*, a suppressor of genome
591 instability, encodes a member of the RecQ helicase/Topo III complex. EMBO J. 24, 2024–

2033. https://doi.org/10.1038/sj.emboj.7600684

Chavez, S., Beilharz, T., Rondón, A.G., Erdjument-Bromage, H., Tempst, P., Svejstrup, J.Q., Lithgow, T., Aguilera, A., 2000. A protein complex containing Tho2, Hpr1, Mft1 and a novel protein, Thp2, connects transcription elongation with mitotic recombination in *Saccharomyces cerevisiae*. EMBO J. 19, 5824–5834. https://doi.org/10.1093/emboj/19.21.5824

Chou, D.M., Elledge, S.J., 2006. Tipin and Timeless form a mutually protective complex required for genotoxic stress resistance and checkpoint function. Proc. Natl. Acad. Sci. U. S. A. 103, 18143–18147. https://doi.org/10.1073/pnas.0609251103

Claussin, C., Chang, M., 2015. The many facets of homologous recombination at telomeres. Microb. Cell 2, 308–321. https://doi.org/10.15698/mic2015.09.224

Claussin, C., Porubský, D., Spierings, D.C.J., Halsema, N., Rentas, S., Guryev, V., Lansdorp, P.M., Chang, M., 2017. Genome-wide mapping of sister chromatid exchange events in single yeast cells using strand-seq. Elife 6, e30560. https://doi.org/10.7554/eLife.30560

Clemente-Ruiz, M., Prado, F., 2009. Chromatin assembly controls replication fork stability. EMBO Rep. 10, 790–796. https://doi.org/10.1038/embor.2009.67

Conover, H.N., Lujan, S.A., Chapman, M.J., Cornelio, D.A., Sharif, R., Williams, J.S., Clark, A.B., Camilo, F., Kunkel, T.A., Argueso, J.L., 2015. Stimulation of chromosomal rearrangements by ribonucleotides. Genetics 201, 951–961. https://doi.org/10.1534/genetics.115.181149

Cornelio, D.A., Sedam, H.N.C., Ferrarezi, J.A., Sampaio, N.M.V., Argueso, J.L., 2017. Both R-loop removal and ribonucleotide excision repair activities of RNase H2 contribute substantially to chromosome stability. DNA Repair (Amst). 52, 110–114. https://doi.org/10.1016/j.dnarep.2017.02.012

Costanzo, M., VanderSluis, B., Koch, E.N., Baryshnikova, A., Pons, C., Tan, G., Wang, W., Usaj, M., Hanchard, J., Lee, S.D., Pelechano, V., Styles, E.B., Billmann, M., Van Leeuwen, J., Van Dyk, N., Lin, Z.Y., Kuzmin, E., Nelson, J., Piotrowski, J.S., Srikumar, T., Bahr, S., Chen, Y., Deshpande, R., Kurat, C.F., Li, S.C., Li, Z., Usaj, M.M., Okada, H., Pascoe, N., Luis, B.J.S., Sharifpoor, S., Shuteriqi, E., Simpkins, S.W., Snider, J., Suresh, H.G., Tan, Y., Zhu, H., Malod-Dognin, N., Janjic, V., Przulj, N., Troyanskaya, O.G., Stagljar, I., Xia, T., Ohya, Y., Gingras, A.C., Raught, B., Boutros, M., Steinmetz, L.M., Moore, C.L., Rosebrock, A.P., Caudy, A.A., Myers, C.L., Andrews, B., Boone, C., 2016. A global genetic interaction network maps a wiring diagram of cellular function. Science (80-.). 353, aaf1420. https://doi.org/10.1126/science.aaf1420

Crow, Y.J., Leitch, A., Hayward, B.E., Garner, A., Parmar, R., Griffith, E., Ali, M., Semple, C., Aicardi, J., Babul-Hirji, R., Baumann, C., Baxter, P., Bertini, E., Chandler, K.E., Chitayat, D., Cau, D., Déry, C., Fazzi, E., Goizet, C., King, M.D., Klepper, J., Lacombe, D., Lanzi, G., Lyall, H., Martínez-Frías, M.L., Mathieu, M., McKeown, C., Monier, A., Oade, Y., Quarrell, O.W., Rittey, C.D., Rogers, R.C., Sanchis, A., Stephenson, J.B.P., Tacke, U., Till, M., Tolmie, J.L., Tomlin, P., Voit, T., Weschke, B., Woods, C.G., Lebon, P., Bonthron,

D.T., Ponting, C.P., Jackson, A.P., 2006. Mutations in genes encoding ribonuclease H2 subunits cause Aicardi-Goutières syndrome and mimic congenital viral brain infection. Nat. Genet. 38, 910–916. https://doi.org/10.1038/ng1842

Datta, A., Adjiri, A., New, L., Crouse, G.F., Jinks Robertson, S., 1996. Mitotic crossovers between diverged sequences are regulated by mismatch repair proteins in *Saccaromyces cerevisiae*. Mol. Cell. Biol. 16, 1085–1093. https://doi.org/10.1128/MCB.16.3.1085

de Wind, N., Dekker, M., Berns, A., Radman, M., te Riele, H., 1995. Inactivation of the mouse Msh2 gene results in mismatch repair deficiency, methylation tolerance, hyperrecombination, and predisposition to cancer. Cell 82, 321–330. https://doi.org/10.1016/0092-8674(95)90319-4

Delaunay, A., Pflieger, D., Barrault, M.-B., Vinh, J., Toledano, M.B., 2002. A thiol peroxidase is an H_2O_2 receptor and redox-transducer in gene activation. Cell 111, 471–481. https://doi.org/10.1016/S0092-8674(02)01048-6

Dittmar, J.C., Pierce, S., Rothstein, R., Reid, R.J.D., 2013. Physical and genetic-interaction density reveals functional organization and informs significance cutoffs in genome-wide screens. Proc Natl Acad Sci U S A 110, 7389–7394. https://doi.org/10.1073/pnas.1219582110

Dittmar, J.C., Reid, R.J.D., Rothstein, R., 2010. ScreenMill: a freely available software suite for growth measurement, analysis and visualization of high-throughput screen data. BMC Bioinformatics 11, 353. https://doi.org/10.1186/1471-2105-11-353

Elliott, B., Jasin, M., 2001. Repair of double-strand breaks by homologous recombination in mismatch repair-defective mammalian cells. Mol. Cell. Biol. 21, 2671–2682. https://doi.org/10.1128/MCB.21.8.2671-2682.2001

Epshtein, A., Potenski, C., Klein, H., 2016. Increased spontaneous recombination in RNase H2-deficient cells arises from multiple contiguous rNMPs and not from single rNMP residues incorporated by DNA polymerase epsilon. Microb. Cell 3, 248–254. https://doi.org/10.15698/mic2016.06.506

Freudenreich, C.H., Su, X.A., 2016. Relocalization of DNA lesions to the nuclear pore complex. FEMS Yeast Res. 16, fow095. https://doi.org/10.1093/femsyr/fow095

George, C.M., Alani, E., 2012. Multiple cellular mechanisms prevent chromosomal rearrangements involving repetitive DNA. Crit. Rev. Biochem. Mol. Biol. 47, 297–313. https://doi.org/10.3109/10409238.2012.675644

Giaever, G., Chu, A.M., Ni, L., Connelly, C., Riles, L., Véronneau, S., Dow, S., Lucau-Danila, A., Anderson, K., André, B., Arkin, A.P., Astromoff, A., El Bakkoury, M., Bangham, R., Benito, R., Brachat, S., Campanaro, S., Curtiss, M., Davis, K., Deutschbauer, A., Entian, K.D., Flaherty, P., Foury, F., Garfinkel, D.J., Gerstein, M., Gotte, D., Güldener, U., Hegemann, J.H., Hempel, S., Herman, Z., Jaramillo, D.F., Kelly, D.E., Kelly, S.L., Kötter, P., LaBonte, D., Lamb, D.C., Lan, N., Liang, H., Liao, H., Liu, L., Luo, C., Lussier, M., Mao, R., Menard, P., Ooi, S.L., Revuelta, J.L., Roberts, C.J., Rose, M., Ross-Macdonald, P.,

Scherens, B., Schimmack, G., Shafer, B., Shoemaker, D.D., Sookhai-Mahadeo, S., Storms, R.K., Strathern, J.N., Valle, G., Voet, M., Volckaert, G., Wang, C. yun, Ward, T.R., Wilhelmy, J., Winzeler, E.A., Yang, Y., Yen, G., Youngman, E., Yu, K., Bussey, H., Boeke, J.D., Snyder, M., Philippsen, P., Davis, R.W., Johnston, M., 2002. Functional profiling of the *Saccharomyces cerevisiae* genome. Nature 418, 387–391. https://doi.org/10.1038/nature00935

Goldfarb, T., Alani, E., 2005. Distinct roles for the *Saccharomyces cerevisiae* mismatch repair proteins in heteroduplex rejection, mismatch repair and nonhomologous tail removal. Genetics 169, 563–574. https://doi.org/10.1534/genetics.104.035204

Hendry, J.A., Tan, G., Ou, J., Boone, C., Brown, G.W., 2015. Leveraging DNA damage response signaling to identify yeast genes controlling genome stability. G3 5, 997–1006. https://doi.org/10.1534/g3.115.016576

Heyer, W.D., 2015. Regulation of recombination and genomic maintenance. Cold Spring Harb. Perspect. Biol. 7, a016501. https://doi.org/10.1101/cshperspect.a016501

Hirata, R., Graham, L.A., Takatsuki, A., Stevens, T.H., Anraku, Y., 1997. *VMA11* and *VMA16* encode second and third proteolipid subunits of the *Saccharomyces cerevisiae* vacuolar membrane H^+-ATPase. J. Biol. Chem. 272, 4795–4803. https://doi.org/10.1074/jbc.272.8.4795

Hishida, T., Iwasaki, H., Ohno, T., Morishita, T., Shinagawa, H., 2001. A yeast gene, *MGS1*, encoding a DNA-dependent AAA+ ATPase is required to maintain genome stability. Proc. Natl. Acad. Sci. 98, 8283–8289. https://doi.org/10.1073/pnas.121009098

Ho, B., Baryshnikova, A., Brown, G.W., 2018. Unification of protein abundance datasets yields a quantitative *Saccharomyces cerevisiae* proteome. Cell Syst. 6, 192–205. https://doi.org/10.1016/j.cels.2017.12.004

Huang, J., Brito, I.L., Villén, J., Gygi, S.P., Amon, A., Moazed, D., 2006. Inhibition of homologous recombination by a cohesin-associated clamp complex recruited to the rDNA recombination enhancer. Genes Dev. 20, 2887–2901. https://doi.org/10.1101/gad.1472706

Huang, M.-E., Kolodner, R.D., 2005. A biological network in *Saccharomyces cerevisiae* prevents the deleterious effects of endogenous oxidative DNA damage. Mol. Cell 17, 709–720. https://doi.org/10.1016/j.molcel.2005.02.008

Huertas, P., Aguilera, A., 2003. Cotranscriptionally formed DNA:RNA hybrids mediate transcription elongation impairment and transcription-associated recombination. Mol. Cell 12, 711–721. https://doi.org/10.1016/j.molcel.2003.08.010

Hughes, A.L., Gottschling, D.E., 2012. An early age increase in vacuolar pH limits mitochondrial function and lifespan in yeast. Nature 492, 261–265. https://doi.org/10.1038/nature11654

Huh, W.-K., Falvo, J. V., Gerke, L.C., Carroll, A.S., Howson, R.W., Weissman, J.S., O'Shea, E.K., 2003. Global analysis of protein localization in budding yeast. Nature 425, 686–691. https://doi.org/10.1038/nature02026

709 Hum, Y.F., Jinks-Robertson, S., 2018. DNA strand-exchange patterns associated with double-
710 strand break-induced and spontaneous mitotic crossovers in *Saccharomyces cerevisiae*.
711 PLoS Genet. 14, e1007302. https://doi.org/10.1371/journal.pgen.1007302

712 Hunter, N., 2015. Meiotic recombination: The essence of heredity. Cold Spring Harb. Perspect.
713 Biol. 7, a016618. https://doi.org/10.1101/cshperspect.a016618

714 Ivessa, A.S., Lenzmeier, B.A., Bessler, J.B., Goudsouzian, L.K., Schnakenberg, S.L., Zakian,
715 V.A., 2003. The *Saccharomyces cerevisiae* helicase Rrm3p facilitates replication past
716 nonhistone protein-DNA complexes. Mol. Cell 12, 1525–1536.
717 https://doi.org/10.1016/S1097-2765(03)00456-8

718 Ivessa, A.S., Zhou, J.Q., Zakian, V.A., 2000. The *Saccharomyces* Pif1p DNA helicase and the
719 highly related Rrm3p have opposite effects on replication fork progression in ribosomal
720 DNA. Cell 100, 479–489. https://doi.org/10.1016/S0092-8674(00)80683-2

721 Johnson, R.D., Jasin, M., 2000. Sister chromatid gene conversion is a prominent double-strand
722 break repair pathway in mammalian cells. EMBO J. 19, 3398–3407.
723 https://doi.org/10.1093/emboj/19.13.3398

724 Kadyk, L.C., Hartwell, L.H., 1992. Sister chromatids are preferred over homologs as substrates
725 for recombinational repair in *Saccharomyces cerevisiae*. Genetics 132, 387–402.
726 https://doi.org/10.1128/EC.3.6.1492

727 Kane, P.M., 2006. The where, when, and how of organelle acidification by the yeast vacuolar
728 H+-ATPase. Microbiol. Mol. Biol. Rev. 70, 177–191.
729 https://doi.org/10.1128/MMBR.70.1.177

730 Katou, Y., Kanoh, Y., Bando, M., Noguchi, H., Tanaka, H., Ashikari, T., Sugimoto, K.,
731 Shirahige, K., 2003. S-phase checkpoint proteins Tof1 and Mrc1 form a stable replication-
732 pausing complex. Nature 424, 1078–1083. https://doi.org/10.1038/nature01900

733 Keil, R.L., McWilliams, A.D., 1993. A gene with specific and global effects on recombination of
734 sequences from tandemly repeated genes in *Saccharomyces cerevisiae*. Genetics 135, 711–
735 718. https://doi.org/10.1016/0168-9525(94)90142-2

736 Kerscher, O., Hieter, P., Winey, M., Basrai, M.A., 2001. Novel role for a *Saccharomyces*
737 *cerevisiae* nucleoporin, Nup170p, in chromosome segregation. Genetics 157, 1543–1553.

738 Keskin, H., Shen, Y., Huang, F., Patel, M., Yang, T., Ashley, K., Mazin, A. V., Storici, F., 2014.
739 Transcript-RNA-templated DNA recombination and repair. Nature 515, 436–439.
740 https://doi.org/10.1038/nature13682

741 Krejci, L., Altmannova, V., Spirek, M., Zhao, X., 2012. Homologous recombination and its
742 regulation. Nucleic Acids Res. 40, 5795–5818. https://doi.org/10.1093/nar/gks270

743 Kuzmin, E., Costanzo, M., Andrews, B., Boone, C., 2016. Synthetic genetic array analysis. Cold
744 Spring Harb. Protoc. 2016, pdb.prot088807. https://doi.org/10.1101/pdb.prot088807

745 Lea, D.E., Coulson, C.A., 1949. The distribution of the numbers of mutants in bacterial

populations. J. Genet. 49, 264–285.

Lehner, K.R., Stone, M.M., Farber, R.A., Petes, T.D., 2007. Ninety-six haploid yeast strains with individual disruptions of Open Reading Frames between *YOR097C* and *YOR192C*, constructed for the *Saccharomyces* Genome Deletion Project, have an additional mutation in the Mismatch Repair gene *MSH3*. Genetics 177, 1951–1953. https://doi.org/10.1534/genetics.107.079368

Leman, A.R., Noguchi, C., Lee, C.Y., Noguchi, E., 2010. Human Timeless and Tipin stabilize replication forks and facilitate sister-chromatid cohesion. J. Cell Sci. https://doi.org/10.1242/jcs.057984

Leuzzi, G., Marabitti, V., Pichierri, P., Franchitto, A., 2016. WRNIP1 protects stalled forks from degradation and promotes fork restart after replication stress. EMBO J. 35, 1437–1451. https://doi.org/10.15252/embj.201593265

Liang, D., Burkhart, S.L., Singh, R.K., Kabbaj, M.H.M., Gunjan, A., 2012. Histone dosage regulates DNA damage sensitivity in a checkpoint-independent manner by the homologous recombination pathway. Nucleic Acids Res. 40, 9604–9620. https://doi.org/10.1093/nar/gks722

López-Flores, I., Garrido-Ramos, M.A., 2012. The repetitive DNA content of eukaryotic genomes. Genome Dyn. 7, 1–28. https://doi.org/10.1159/000337118

Luria, S.E., Delbrück, M., 1943. Mutations of bacteria from virus sensitivity to virus resistance. Genetics 28, 491–511.

Mayer, M.L., Pot, I., Chang, M., Xu, H., Aneliunas, V., Kwok, T., Newitt, R., Aebersold, R., Boone, C., Brown, G.W., Hieter, P., 2004. Identification of protein complexes required for efficient sister chromatid cohesion. Mol. Biol. Cell 15, 1736–1745. https://doi.org/10.1091/mbc.E03-08-0619

McVey, M., Khodaverdian, V.Y., Meyer, D., Cerqueira, P.G., Heyer, W.-D., 2016. Eukaryotic DNA polymerases in homologous recombination. Annu. Rev. Genet. 50, 393–421. https://doi.org/10.1146/annurev-genet-120215-035243

Mekhail, K., Seebacher, J., Gygi, S.P., Moazed, D., 2008. Role for perinuclear chromosome tethering in maintenance of genome stability. Nature 456, 667–670. https://doi.org/10.1038/nature07460

Milgrom, E., Diab, H., Middleton, F., Kane, P.M., 2007. Loss of vacuolar proton-translocating ATPase activity in yeast results in chronic oxidative stress. J. Biol. Chem. 282, 7125–7136. https://doi.org/10.1074/jbc.M608293200

Mohanty, B.K., Bairwa, N.K., Bastia, D., 2006. The Tof1p-Csm3p protein complex counteracts the Rrm3p helicase to control replication termination of *Saccharomyces cerevisiae*. Proc. Natl. Acad. Sci. U. S. A. 103, 897–902. https://doi.org/10.1073/pnas.0506540103

Morano, K.A., Grant, C.M., Moye-Rowley, W.S., 2012. The response to heat shock and oxidative stress in *Saccharomyces cerevisiae*. Genetics 190, 1157–1195.

https://doi.org/10.1534/genetics.111.128033

Myung, K., Datta, A., Chen, C., Kolodner, R.D., 2001. *SGS1*, the *Saccharomyces cerevisiae* homologue of BLM and WRN, suppresses genome instability and homeologous recombination. Nat. Genet. 27, 113–116. https://doi.org/10.1038/83673

Nicholson, A., Hendrix, M., Jinks-Robertson, S., Crouse, G.F., 2000. Regulation of mitotic homeologous recombination in yeast: functions of mismatch repair and nucleotide excision repair genes. Genetics 154, 133–146.

Noguchi, E., Noguchi, C., Du, L.-L., Russell, P., 2003. Swi1 prevents replication fork collapse and controls checkpoint kinase Cds1. Mol. Cell. Biol. 23, 7861–7874. https://doi.org/10.1128/MCB.23.21.7861-7874.2003

Noguchi, E., Noguchi, C., McDonald, W.H., Yates, J.R., Russell, P., 2004. Swi1 and Swi3 are components of a Replication Fork Protection Complex in fission yeast. Mol. Cell. Biol. 24, 8342–8355. https://doi.org/10.1128/MCB.24.19.8342-8355.2004

Novarina, D., Janssens, G.E., Bokern, K., Schut, T., van Oerle, N.C., Kazemier, H.G., Veenhoff, L.M., Chang, M., 2020. A genome-wide screen identifies genes that suppress the accumulation of spontaneous mutations in young and aged yeast cells. Aging Cell 19, e13084. https://doi.org/10.1111/acel.13084

O'Connell, K., Jinks-Robertson, S., Petes, T.D., 2015. Elevated Genome-wide instability in yeast mutants lacking RNase H activity. Genetics 201, 963–975. https://doi.org/10.1534/genetics.115.182725

Owiti, N., Lopez, C., Singh, S., Stephenson, A., Kim, N., 2017. Def1 and Dst1 play distinct roles in repair of AP lesions in highly transcribed genomic regions. DNA Repair (Amst). 55, 31–39. https://doi.org/10.1016/j.dnarep.2017.05.003

Pan, X., Ye, P., Yuan, D.S., Wang, X., Bader, J.S., Boeke, J.D., 2006. A DNA integrity network in the yeast *Saccharomyces cerevisiae*. Cell 124, 1069–1081. https://doi.org/10.1016/j.cell.2005.12.036

Poon, B.P.K., Mekhail, K., 2011. Cohesin and related coiled-coil domain-containing complexes physically and functionally connect the dots across the genome. Cell Cycle 10, 2669–2682. https://doi.org/10.4161/cc.10.16.17113

Popoff, S.C., Spira, A.I., Johnson, A.W., Demple, B., 1990. Yeast structural gene (*APN1*) for the major apurinic endonuclease: homology to *Escherichia coli* endonuclease IV. Proc. Natl. Acad. Sci. U. S. A. 87, 4193–4197. https://doi.org/10.1073/pnas.87.11.4193

Potenski, C.J., Niu, H., Sung, P., Klein, H.L., 2014. Avoidance of ribonucleotide-induced mutations by RNase H2 and Srs2-Exo1 mechanisms. Nature 511, 251–254. https://doi.org/10.1038/nature13292

Prado, F., Aguilera, A., 2005. Partial depletion of histone H4 increases homologous recombination-mediated genetic instability. Mol. Cell. Biol. 25, 1526–1536. https://doi.org/10.1128/mcb.25.4.1526-1536.2005

Prakash, S., Prakash, L., 2000. Nucleotide excision repair in yeast. Mutat. Res. 451, 13–24. https://doi.org/10.1016/S0027-5107(00)00037-3

Saugar, I., Parker, J.L., Zhao, S., Ulrich, H.D., 2012. The genome maintenance factor Mgs1 is targeted to sites of replication stress by ubiquitylated PCNA. Nucleic Acids Res. 40, 245–257. https://doi.org/10.1093/nar/gkr738

Schalbetter, S.A., Mansoubi, S., Chambers, A.L., Downs, J.A., Baxter, J., 2015. Fork rotation and DNA precatenation are restricted during DNA replication to prevent chromosomal instability. Proc. Natl. Acad. Sci. 112, E4565–E4570. https://doi.org/10.1073/pnas.1505356112

Schmidt, K.H., Kolodner, R.D., 2004. Requirement of Rrm3 helicase for repair of spontaneous DNA lesions in cells lacking Srs2 or Sgs1 helicase. Mol. Cell. Biol. 24, 3213–3226. https://doi.org/10.1128/MCB.24.8.3213

Schneider, C.A., Rasband, W.S., Eliceiri, K.W., 2012. NIH Image to ImageJ : 25 years of image analysis. Nat. Methods 9, 671–675. https://doi.org/10.1038/nmeth.2089

Sherman, F., 2002. Getting started with yeast. Methods Enzymol. 350, 3–41. https://doi.org/http://dx.doi.org/10.1016/S0076-6879(02)50954-X

Smith, J., Rothstein, R., 1999. An allele of *RFA1* suppresses *RAD52*-dependent double-strand break repair in *Saccharomyces cerevisiae*. Genetics 151, 447–458.

Sommariva, E., Pellny, T.K., Karahan, N., Kumar, S., Huberman, J.A., Dalgaard, J.Z., 2005. *Schizosaccharomyces pombe* Swi1, Swi3, and Hsk1 are components of a novel S-phase response pathway to alkylation damage. Mol. Cell. Biol. 25, 2770–2784. https://doi.org/10.1128/MCB.25.7.2770-2784.2005

Spell, R.M., Jinks-Robertson, S., 2004. Examination of the roles of Sgs1 and Srs2 helicases in the enforcement of recombination fidelity in *Saccharomyces cerevisiae*. Genetics 168, 1855–1865. https://doi.org/10.1534/genetics.104.032771

Spies, M., Fishel, R., 2015. Mismatch repair during homologous and homeologous recombination. Cold Spring Harb. Perspect. Biol. 7, a022657. https://doi.org/10.1101/cshperspect.a022657

Stirling, P.C., Bloom, M.S., Solanki-Patil, T., Smith, S., Sipahimalani, P., Li, Z., Kofoed, M., Ben-Aroya, S., Myung, K., Hieter, P., 2011. The complete spectrum of yeast chromosome instability genes identifies candidate CIN cancer genes and functional roles for ASTRA complex components. PLoS Genet. 7, e1002057. https://doi.org/10.1371/journal.pgen.1002057

Styles, E.B., Founk, K.J., Zamparo, L.A., Sing, T.L., Altintas, D., Ribeyre, C., Ribaud, V., Rougemont, J., Mayhew, D., Costanzo, M., Usaj, M., Verster, A.J., Koch, E.N., Novarina, D., Graf, M., Luke, B., Muzi-Falconi, M., Myers, C.L., Mitra, R.D., Shore, D., Brown, G.W., Zhang, Z., Boone, C., Andrews, B.J., 2016. Exploring quantitative yeast phenomics with single-cell analysis of DNA damage foci. Cell Syst. 3, 264-277.e10.

Sugawara, N., Goldfarb, T., Studamire, B., Alani, E., Haber, J.E., 2004. Heteroduplex rejection during single-strand annealing requires Sgs1 helicase and mismatch repair proteins Msh2 and Msh6 but not Pms1. Proc. Natl. Acad. Sci. U. S. A. 101, 9315–9320. https://doi.org/10.1073/pnas.0305749101

Supek, F., Bošnjak, M., Škunca, N., Šmuc, T., 2011. REVIGO summarizes and visualizes long lists of Gene Ontology terms. PLoS One 6, e21800. https://doi.org/10.1371/journal.pone.0021800

Swanson, R.L., Morey, N.J., Doetsch, P.W., Jinks-Robertson, S., 1999. Overlapping specificities of base excision repair, nucleotide excision repair, recombination, and translesion synthesis pathways for DNA base damage in *Saccharomyces cerevisiae*. Mol. Cell. Biol. 19, 2929–2935. https://doi.org/10.1128/MCB.19.4.2929

Symington, L.S., Rothstein, R., Lisby, M., 2014. Mechanisms and regulation of mitotic recombination in *Saccharomyces cerevisiae*. Genetics 198, 795–835. https://doi.org/10.1534/genetics.114.166140

Thorpe, G.W., Fong, C.S., Alic, N., Higgins, V.J., Dawes, I.W., 2004. Cells have distinct mechanisms to maintain protection against different reactive oxygen species: Oxidative-stress-response genes. Proc. Natl. Acad. Sci. 101, 6564–6569. https://doi.org/10.1073/pnas.0305888101

Torres, J.Z., Schnakenberg, S.L., Zakian, V.A., 2004. *Saccharomyces cerevisiae* Rrm3p DNA helicase promotes genome integrity by preventing replication fork stalling: viability of *rrm3* cells requires the intra-S-phase checkpoint and fork restart activities. Mol. Cell. Biol. 24, 3198–3212. https://doi.org/10.1128/MCB.24.8.3198-3212.2004

Treco, D.A., Lundblad, V., 2001. Preparation of yeast media. Curr. Protoc. Mol. Biol. Chapter 13, Unit13.1. https://doi.org/10.1002/0471142727.mb1301s23

Tsurimoto, T., Shinozaki, A., Yano, M., Seki, M., Enomoto, T., 2005. Human Werner helicase interacting protein 1 (WRNIP1) functions as novel modulator for DNA polymerase δ. Genes to Cells 10, 13–22. https://doi.org/10.1111/j.1365-2443.2004.00812.x

Ulrich, H.D., 2005. The *RAD6* pathway: Control of DNA damage bypass and mutagenesis by ubiquitin and SUMO. ChemBioChem 6, 1735–1743. https://doi.org/10.1002/cbic.200500139

Umemoto, N., Ohya, Y., Anraku, Y., 1991. *VMA11*, a novel gene that encodes a putative proteolipid, is indispensable for expression of yeast vacuolar membrane H^+-ATPase activity. J. Biol. Chem. 266, 24526–24532.

Urtishak, K.A., Smith, K.D., Chanoux, R.A., Greenberg, R.A., Johnson, F.B., Brown, E.J., 2009. Timeless maintains genomic stability and suppresses sister chromatid exchange during unperturbed DNA replication. J. Biol. Chem. 284, 8777–8785. https://doi.org/10.1074/jbc.M806103200

Usaj, M., Tan, Y., Wang, W., VanderSluis, B., Zou, A., Myers, C.L., Costanzo, M., Andrews, B., Boone, C., 2017. TheCellMap.org: a web-accessible database for visualizing and mining the

global yeast genetic interaction network. G3 (Bethesda). 7, 1539–1549. https://doi.org/10.1534/g3.117.040220

Vance, J.R., Wilson, T.E., 2001. Repair of DNA strand breaks by the overlapping functions of lesion-specific and non-lesion-specific DNA 3' phosphatases. Mol. Cell. Biol. 21, 7191–7198. https://doi.org/10.1128/MCB.21.21.7191-7198.2001

Veatch, J.R., McMurray, M.A., Nelson, Z.W., Gottschling, D.E., 2009. Mitochondrial dysfunction leads to nuclear genome instability via an iron-sulphur cluster defect. Cell 137, 1247–1258. https://doi.org/10.1016/j.cell.2009.04.014

Warde-Farley, D., Donaldson, S.L., Comes, O., Zuberi, K., Badrawi, R., Chao, P., Franz, M., Grouios, C., Kazi, F., Lopes, C.T., Maitland, A., Mostafavi, S., Montojo, J., Shao, Q., Wright, G., Bader, G.D., Morris, Q., 2010. The GeneMANIA prediction server: biological network integration for gene prioritization and predicting gene function. Nucleic Acids Res. 38, W214-220. https://doi.org/10.1093/nar/gkq537

Wong, C.M., Siu, K.L., Jin, D.Y., 2004. Peroxiredoxin-null yeast cells are hypersensitive to oxidative stress and are genomically unstable. J. Biol. Chem. 279, 23207–23213. https://doi.org/10.1074/jbc.M402095200

Wu, L., Bachrati, C.Z., Ou, J., Xu, C., Yin, J., Chang, M., Wang, W., Li, L., Brown, G.W., Hickson, I.D., 2006. BLAP75/RMI1 promotes the BLM-dependent dissolution of homologous recombination intermediates. Proc. Natl. Acad. Sci. 103, 4068–4073. https://doi.org/10.1073/pnas.0508295103

Xia, L., Jaafar, L., Cashikar, A., Flores-Rozas, H., 2007. Identification of genes required for protection from doxorubicin by a genome-wide screen in *Saccharomyces cerevisiae*. Cancer Res. 67, 11411–11418. https://doi.org/10.1158/0008-5472.CAN-07-2399

Xiao, W., Samson, L., 1993. In vivo evidence for endogenous DNA alkylation damage as a source of spontaneous mutation in eukaryotic cells. Proc. Natl. Acad. Sci. U. S. A. 90, 2117–2121. https://doi.org/10.1073/pnas.90.6.2117

Xu, H., Boone, C., Klein, H.L., 2004. Mrc1 is required for sister chromatid cohesion to aid in recombination repair of spontaneous damage. Mol. Cell. Biol. 24, 7082–7090. https://doi.org/10.1128/MCB.24.16.7082-7090.2004

Yang, J., Bachrati, C.Z., Ou, J., Hickson, I.D., Brown, G.W., 2010. Human topoisomerase IIIα is a single-stranded DNA decatenase that is stimulated by BLM and RMI1. J. Biol. Chem. 285, 21426–21436. https://doi.org/10.1074/jbc.M110.123216

Yi, D.G., Kim, M.J., Choi, J.E., Lee, J., Jung, J., Huh, W.K., Chung, W.H., 2016. Yap1 and Skn7 genetically interact with Rad51 in response to oxidative stress and DNA double-strand break in *Saccharomyces cerevisiae*. Free Radic. Biol. Med. 101, 424–433. https://doi.org/10.1016/j.freeradbiomed.2016.11.005

Zhang, C., 2014. Essential functions of iron-requiring proteins in DNA replication, repair and cell cycle control. Protein Cell 5, 750–760. https://doi.org/10.1007/s13238-014-0083-7

937

938 FIGURE LEGENDS

939

940 **Figure 1. A genome-wide patching and replica plating screen for mutants with increased**
941 **direct-repeat recombination.**

942 (**A**) The *leu2* direct-repeat recombination assay. Spontaneous recombination between two *leu2*
943 heteroalleles, either through gene conversion or intra-chromosomal single strand annealing
944 (SSA), yields a functional *LEU2* gene. (**B**) Schematic representation of the screen based on
945 patching and replica plating. The *leu2* direct-repeat recombination cassette was introduced into
946 the yeast deletion collection (YKO) by crossing the collection with a query strain containing the
947 cassette. Haploid strains containing each gene deletion and the recombination cassette were
948 isolated using SGA methodology. Each strain was patched on rich medium and replica-plated to
949 selective medium, where hyper-recombinant mutants form papillae on the surface of the patch.
950 Recombination rates were measured for positives from the patch assay using fluctuation tests. (**C**)
951 Example plates from the patch assay. Each plate bears a negative control (wild type) and a
952 positive control (*elg1*Δ). Two positive hits from the screen (*rad4*Δ, *ydl162c*Δ) are shown. (**D**)
953 Recombination rates are plotted for the validated positives from the patch screen, alongside the
954 wild-type strain. Each data point is from an independent fluctuation test, with n≥3 for each strain.
955 The vertical bars indicate the mean recombination rate for each strain. (**E**) The top 10 statistically
956 supported GO terms enriched in the hits from the patch assay screen are shown, with the -fold
957 enrichment for each term.

958

959 **Figure 2. A high-throughput replica-pinning screen for genes controlling direct-repeat**
960 **recombination.**

(**A**) Schematic representation of the screen based on high-throughput replica-pinning. The *leu2* direct-repeat recombination cassette was introduced into the yeast deletion collection as in Figure 1B. The resulting strains were amplified by parallel high-throughput replica pinning and subsequently replica-pinned to media lacking leucine to select for recombination events. Recombination frequencies were calculated for each strain of the YKO collection. (**B**) Recombination frequency distribution for the YKO collection (*MSH3* strains) and for the *msh3* strains in the collection. Recombination frequencies for a wild-type and for a recombination-defective *rad54*Δ strain derived from a pilot experiment are indicated by the dashed lines. (**C**) Interaction densities determined by CLIK analysis are plotted as a two-dimensional heatmap. The cutoffs established by CLIK analysis for hyper-recombination (hyper-rec) and recombination-defective (hypo-rec) genes are shown in the insets. (**D**) The statistically supported GO terms enriched in the hits from the pinning assay screen are shown, with the enrichment for each term. (**E**) Recombination rates from fluctuation tests of *csm1*Δ and *nup170*Δ are plotted. Each data point is from an independent fluctuation test, with n=3 for each strain. The vertical bars indicate the mean recombination rate for each strain and the wild-type data from Figure 1D are plotted for comparison.

Figure 3. Functional analysis of validated hyper-rec genes.

(A) The overlap of the hyper-rec genes for the two screens is plotted as a Venn diagram. The 15 genes identified in both screens are indicated. **(B)** A protein-protein interaction network for the proteins encoded by the 35 validated hyper-rec genes is shown. Nodes represent the proteins, and are colored to indicate function. Edges indicate a physical interaction as annotated in the GeneMania database. **(C)** Spatial analysis of functional enrichment. On the left, the yeast genetic interaction similarity network is annotated with GO biological process terms to identify major

functional domains (Costanzo et al. 2016). 11 of the 17 domains are labeled and delineated by coloured outlines. On the right, the network is annotated with the 35 validated hyper-rec genes. The overlay indicates the functional domains annotated on the left. Only nodes with statistically supported enrichments (SAFE score > 0.08, $p < 0.05$) are coloured. (**D**) The 35 validated hyper-rec genes are compared with existing *Saccharomyces* Genome Database annotations and genome instability datasets that measured Rad52 focus formation (Alvaro et al., 2007; Styles et al., 2016), *RNR3* induction (Hendry et al., 2015), or chromosome instability (CIN; (Stirling et al., 2011)). A green bar indicates that the gene has the given annotation or was detected in the indicated screen.

Figure 4. Spatial analysis of functional enrichment for four hyper-rec genes. The genetic interactions of each of the indicated genes was tested for enrichments in the functional neighbourhoods of the yeast genetic interaction similarity network. The overlay indicates a subset of functional domains as annotated on Figure 3C. Nodes with statistically supported enrichments (Neighbourhood enrichment $p < 0.05$) are coloured, black for negative genetic interactions and red for positive genetic interactions.

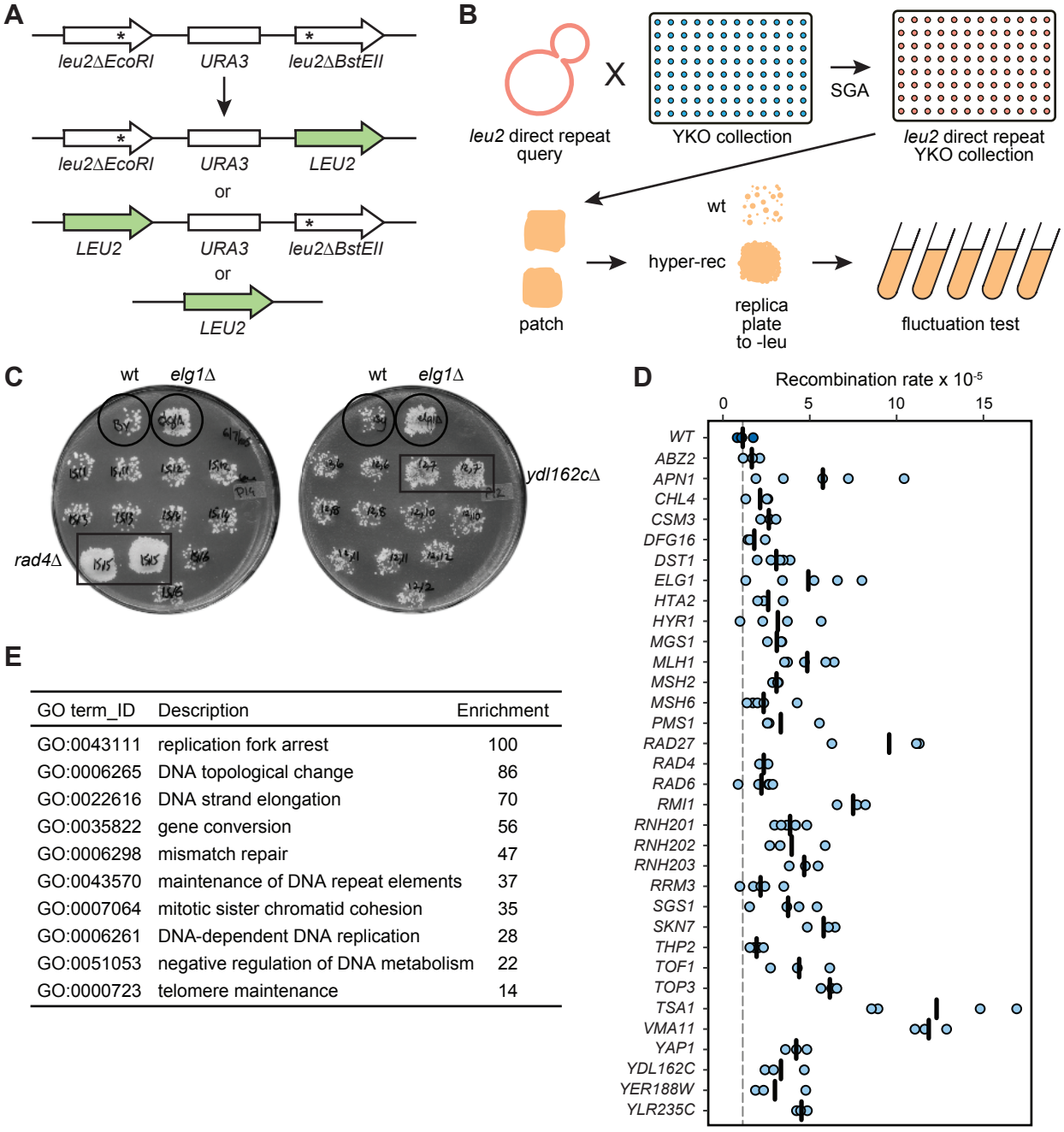

E

GO term_ID	Description	Enrichment
GO:0043111	replication fork arrest	100
GO:0006265	DNA topological change	86
GO:0022616	DNA strand elongation	70
GO:0035822	gene conversion	56
GO:0006298	mismatch repair	47
GO:0043570	maintenance of DNA repeat elements	37
GO:0007064	mitotic sister chromatid cohesion	35
GO:0006261	DNA-dependent DNA replication	28
GO:0051053	negative regulation of DNA metabolism	22
GO:0000723	telomere maintenance	14

Figure 1. A genome-wide patching and replica plating screen for mutants with increased direct-repeat recombination. (A) The *leu2* direct-repeat recombination assay. Spontaneous recombination between two *leu2* heteroalleles, either through gene conversion or intra-chromosomal single strand annealing (SSA), yields a functional *LEU2* gene. **(B)** Schematic representation of the screen based on patching and replica plating. The *leu2* direct-repeat recombination cassette was introduced into the yeast deletion collection (YKO) by crossing the collection with a query strain containing the cassette. Haploid strains containing each gene deletion and the recombination cassette were isolated using SGA methodology. Each strain was patched on rich medium and replica-plated to selective medium, where hyper-recombinant mutants form papillae on the surface of the patch. Recombination rates were measured for positives from the patch assay using fluctuation tests. **(C)** Example plates from the patch assay. Each plate bears a negative control (wild type) and a positive control (*elg1*Δ). Two positive hits from the screen (*rad4*Δ, *ydl162c*Δ) are shown. **(D)** Recombination rates are plotted for the validated positives from the patch screen, alongside the wild-type strain. Each data point is from an independent fluctuation test, with n≥3 for each strain. The vertical bars indicate the mean recombination rate for each strain. **(E)** The top 10 statistically supported GO terms enriched in the hits from the patch assay screen are shown, with the -fold enrichment for each term.

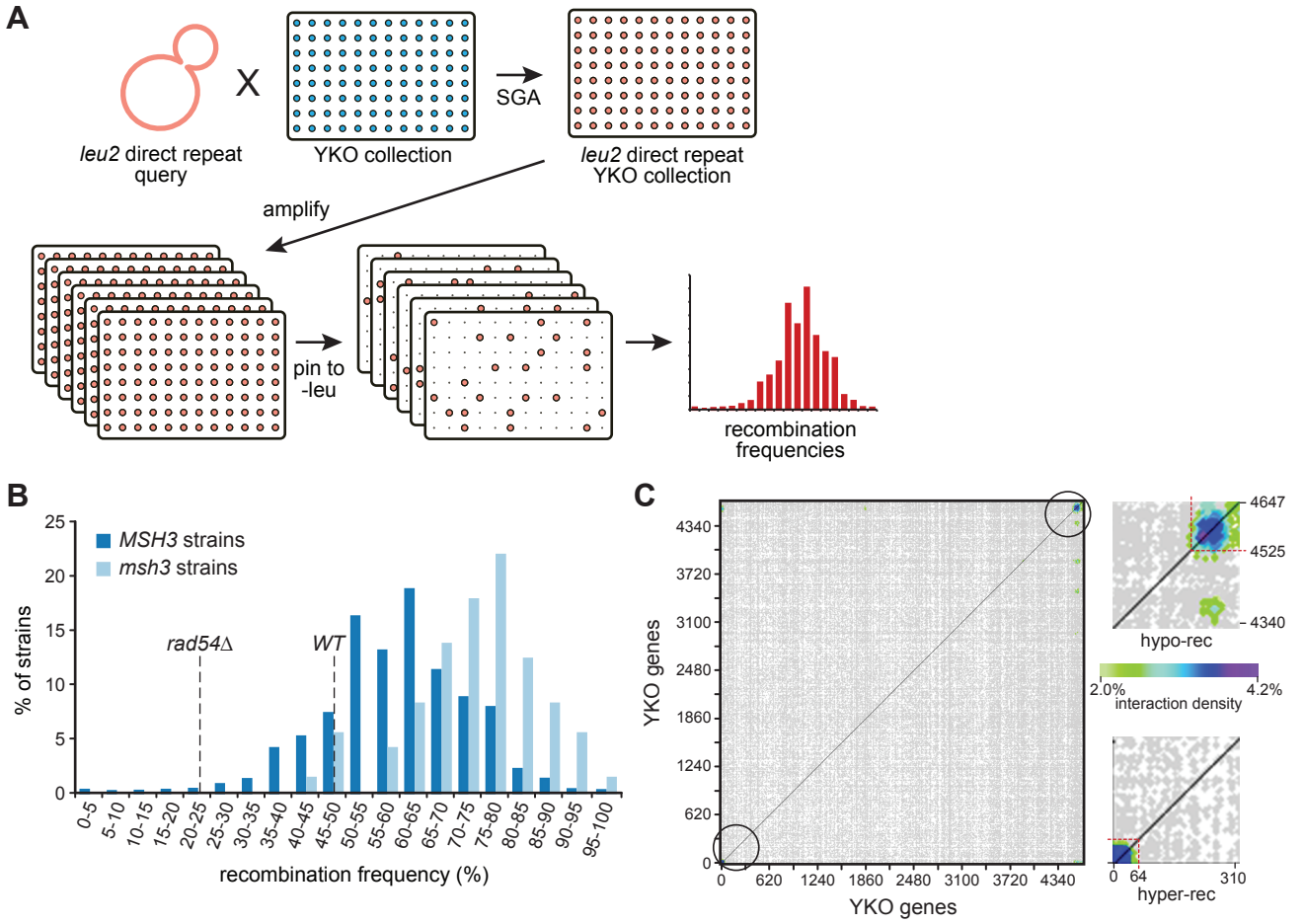

GO term_ID	Description	Enrichment
GO:0043137	DNA replication, primer removal	55
GO:0022616	DNA strand elongation	26
GO:0006261	DNA-dependent DNA replication	8
GO:0006281	DNA repair	5
GO:0006974	cellular response to DNA damage	4
GO:0006259	DNA metabolism	4

Figure 2. A high-throughput replica-pinning screen for genes controlling direct-repeat recombination. (A) Schematic representation of the screen based on high-throughput replica-pinning. The *leu2* direct-repeat recombination cassette was introduced into the yeast deletion collection as in Figure 1B. The resulting strains were amplified by parallel high-throughput replica pinning and subsequently replica-pinned to media lacking leucine to select for recombination events. Recombination frequencies were calculated for each strain of the YKO collection. **(B)** Recombination frequency distribution for the YKO collection (*MSH3* strains) and for the *msh3* strains in the collection. Recombination frequencies for a wild-type and for a recombination-defective *rad54*Δ strain derived from a pilot experiment are indicated by the dashed lines. **(C)** Interaction densities determined by CLIK analysis are plotted as a two-dimensional heatmap. The cutoffs established by CLIK analysis for hyper-recombination (hyper-rec) and recombination-defective (hypo-rec) genes are shown in the insets. **(D)** The statistically supported GO terms enriched in the hits from the pinning assay screen are shown, with the enrichment for each term. **(E)** Recombination rates from fluctuation tests of csm1Δ and nup170Δ are plotted. Each data point is from an independent fluctuation test, with n=3 for each strain. The vertical bars indicate the mean recombination rate for each strain and the wild-type data from Figure 1D are plotted for comparison.

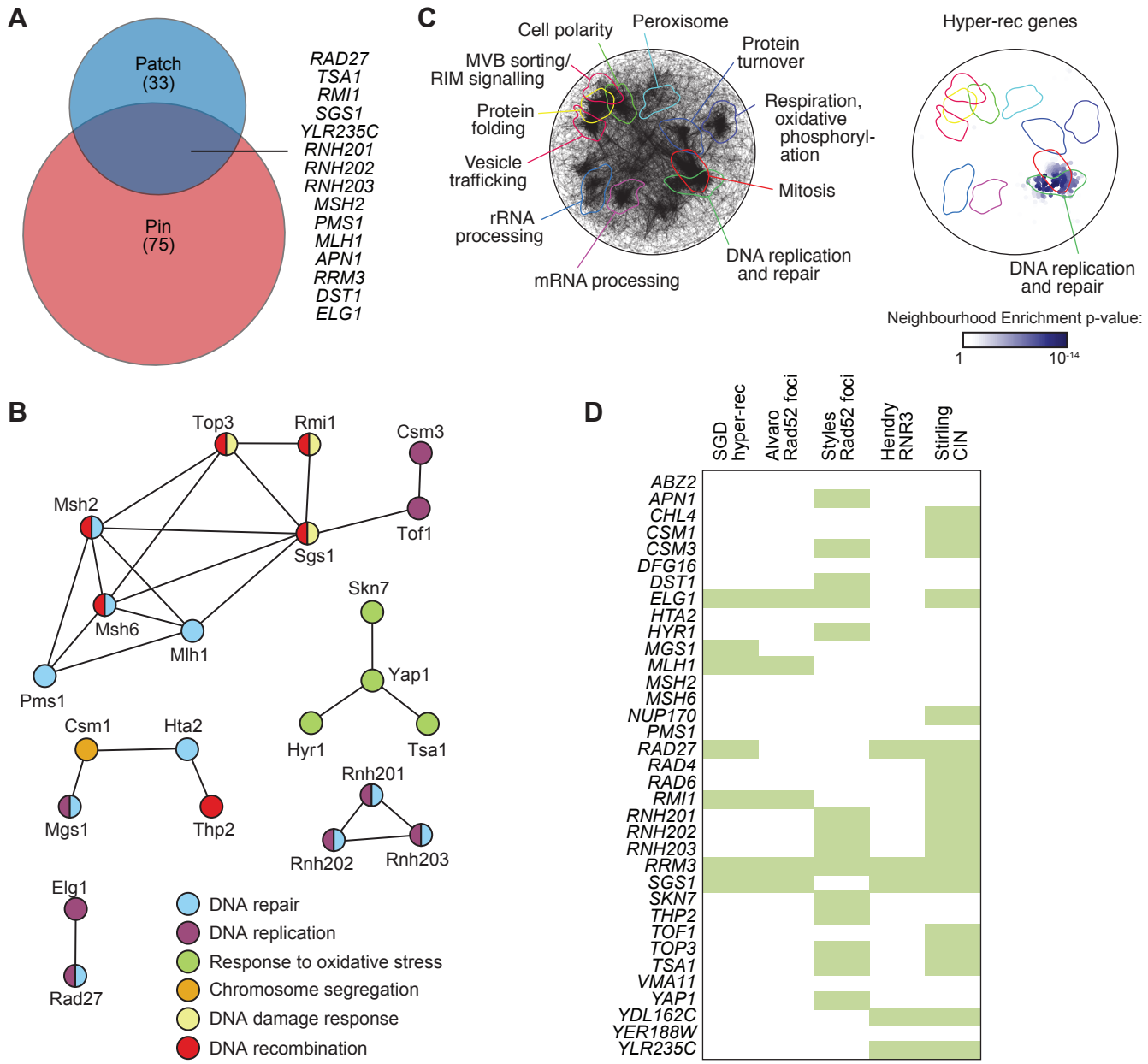

Figure 3. Functional analysis of validated hyper-rec genes. (A) The overlap of the hyper-rec genes for the two screens is plotted as a Venn diagram. The 15 genes identified in both screens are indicated. **(B)** A protein-protein interaction network for the proteins encoded by the 35 validated hyper-rec genes is shown. Nodes represent the proteins, and are colored to indicate function. Edges indicate a physical interaction as annotated in the GeneMania database. **(C)** Spatial analysis of functional enrichment. On the left, the yeast genetic interaction similarity network is annotated with GO biological process terms to identify major functional domains (Costanzo et al., 2016). 11 of the 17 domains are labeled and delineated by coloured outlines. On the right, the network is annotated with the 35 validated hyper-rec genes. The overlay indicates the functional domains annotated on the left. Only nodes with statistically supported enrichments (SAFE score > 0.08, $p < 0.05$) are coloured. **(D)** The 35 validated hyper-rec genes are compared with existing Saccharomyces Genome Database annotations and genome instability datasets that measured Rad52 focus formation (Alvaro et al., 2007; Styles et al., 2016), RNR3 induction (Hendry et al., 2015), or chromosome instability (CIN; (Stirling et al., 2011)). A green bar indicates that the gene has the given annotation or was detected in the indicated screen.

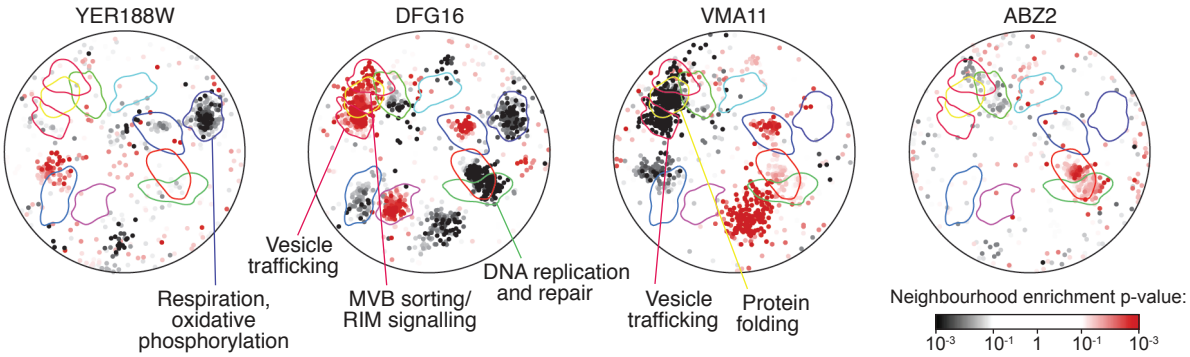

Figure 4. Spatial analysis of functional enrichment for four hyper-rec genes. The genetic interactions of each of the indicated genes was tested for enrichments in the functional neighbourhoods of the yeast genetic interaction similarity network. The overlay indicates a subset of functional domains as annotated on Figure 3C. Nodes with statistically supported enrichments (Neighbourhood enrichment $p < 0.05$) are coloured, black for negative genetic interactions and red for positive genetic interactions.

Table 1. Hyper-recombination genes from the patch assay and pinning assay screens.

Patch Assay				Pinning Assay Hyper-Rec			
Gene name	Mean recombination rate[a]	Standard deviation	p-value[b]	Gene name	Recombinant colonies (%)	Gene name	Recombinant colonies (%)
WT	1.14E-05	2.84E-06		*CSM1*	100	*RNH201*	90
TSA1	1.23E-04	3.64E-05	7.76E-05	*ELG1*	100	*YGL159W*	90
VMA11	1.19E-04	7.62E-06	1.27E-08	*MSH2*	100	*YJL043W*	90
RAD27	9.39E-05	2.59E-05	1.26E-04	*RAD27*	100	*YLR279W*	90
RMI1	7.50E-05	6.85E-06	2.65E-07	*RRM3*	100	*YOR082C*	90
TOP3	6.15E-05	3.80E-06	1.13E-07	*SGS1*	100	*ARP8*	88
SKN7	5.80E-05	6.85E-06	2.20E-06	*TSA1*	100	*BIO3*	88
APN1	5.75E-05	2.97E-05	3.79E-03	*DST1*	98	*COX7*	88
ELG1	5.09E-05	1.30E-05	1.73E-04	*RNH202*	98	*DCS2*	88
MLH1	4.86E-05	1.15E-05	3.43E-05	*RNH203*	98	*DDC1*	88
RNH203	4.68E-05	6.79E-06	1.31E-05	*MLH1*	96	*FUS2*	88
YLR235C	4.52E-05	2.57E-06	6.11E-07	*NUP170*	96	*HST3*	88
TOF1	4.39E-05	1.40E-05	9.45E-04	*PMS1*	96	*KIP1*	88
YAP1	4.22E-05	5.04E-06	8.67E-06	*ALE1*	94	*MFT1*	88
RNH202	3.96E-05	1.38E-05	1.96E-03	*APN1*	94	*MNT2*	88
RNH201	3.86E-05	6.08E-06	1.91E-06	*NFI1*	94	*MRPL51*	88
SGS1	3.75E-05	1.42E-05	2.25E-03	*YGR117C*	94	*NIT3*	88
YDL162C	3.34E-05	9.73E-06	1.38E-03	*YML020W*	94	*PCL10*	88
PMS1	3.33E-05	1.28E-05	3.46E-03	*YMR166C*	94	*PET123*	88
HYR1	3.16E-05	1.74E-05	1.85E-02	*YOR072W*	94	*PHM8*	88
MGS1	3.10E-05	3.83E-06	6.14E-05	*RPL23a*	94	*REC114*	88
MSH2	3.09E-05	1.34E-06	1.55E-06	*DIA2*	92	*RGS2*	88
DST1	3.07E-05	6.56E-06	1.15E-04	*EFT1*	92	*SCO1*	88
YER188W	2.99E-05	1.27E-05	9.90E-03	*MDM1*	92	*SPR1*	88

CSM3	2.64E-05	3.65E-06	2.78E-04	*MSN4*	92	*TOM5*	88
HTA2	2.60E-05	6.24E-06	1.87E-03	*PNS1*	92	*ULS1*	88
RAD4	2.35E-05	2.46E-06	1.73E-03	*RMI1*	92	*YDL009C*	88
MSH6	2.34E-05	1.02E-05	1.68E-02	*RRT14*	92	*YEL020C*	88
RAD6	2.22E-05	7.25E-06	7.23E-03	*SAC3*	92	*YGL042C*	88
RRM3	2.16E-05	8.30E-06	1.54E-02	*YDR230W*	92	*YJL017W*	88
CHL4	2.14E-05	5.86E-06	9.36E-03	*YLR235C*	92	*YJR018W*	88
THP2	1.94E-05	2.95E-06	2.52E-03	*YNL122C*	92	*YJR124C*	88
DFG16	1.80E-05	4.48E-06	2.44E-02	*YTA7*	92	*YKL091C*	88
ABZ2	1.66E-05	3.93E-06	4.25E-02	*FSH1*	90	*YKL162C*	88
				GET3	90	*YNL179C*	88
				KGD2	90	*YOR309C*	88
				MID2	90	*YOR333C*	88
				POL32	90		

[a] Recombination rate from Table S2

[b] p-values from one-sided Student's *t*-test

Table 2. Hypo-recombination genes from the pinning assay screen.

Pinning Assay Hypo-Rec							
Gene name	**Recombinant colonies (%)**	**Gene name**	**Recombinant colonies (%)**	**Gene name**	**Recombinant colonies (%)**	**Gene name**	**Recombinant colonies (%)**
YCL021W-A	0.0	*SIP3*	17.2	*HST4*	27.1	*AIM39*	31.3
YEL045C	0.0	*BEM1*	18.8	*PHO85*	27.1	*CIK1*	31.3
GLY1	0.0	*BUB3*	18.8	*PRM4*	27.1	*HOL1*	31.3
HIS5	0.0	*OPI3*	18.8	*RIM1*	27.1	*MET22*	31.3
RAD52	2.1	*YER038W-A*	18.9	*UBP15*	27.1	*SWH1*	31.3
GCN4	2.9	*ARG7*	19.1	*VMA21*	27.1	*RNR4*	31.3
CYS4	3.1	*LIN1*	19.6	*YBR075W*	27.1	*RPN4*	31.3
POS5	3.1	*OPY2*	20.0	*AAT2*	27.5	*RPS18B*	31.3
REC104	4.2	*HEF3*	20.0	*RAD50*	27.8	*TSL1*	31.3
YHR080C	4.2	*DAL81*	20.9	*ARG2*	28.1	*VPS60*	31.3
ATP15	4.8	*YLR361C-A*	21.3	*IRE1*	28.2	*VTH1*	31.3
YPR099C	4.9	*RPL22A*	21.6	*PDR16*	28.2	*YKE2*	31.3
YOR302W	5.3	*RSM7*	21.7	*RNR1*	28.2	*YNR040W*	31.3
ACO2	6.4	*CCR4*	22.2	*YKR023W*	28.6	*NUP84*	31.6
MDM20	6.4	*LOC1*	22.2	*ATP1*	29.2	*BOI1*	31.7
MDM10	6.9	*AHC1*	22.9	*FIT2*	29.2	*URA2*	31.7
NPL3	7.1	*CIN1*	22.9	*HSP42*	29.2	*RTC3*	31.8
HIS7	7.7	*VRP1*	22.9	*RAD54*	29.2	*THP1*	31.8
FUN12	8.3	*YEL014C*	22.9	*RAD55*	29.2	*BUD20*	32.1
BDF1	11.1	*CDC40*	23.1	*SNO1*	29.2	*RPS16A*	32.6
YNL011C	12.5	*MDM34*	23.4	*SPE2*	29.2		
SWI6	12.8	*OST4*	23.5	*SPT21*	29.2		
URA1	13.2	*YOL013W-B*	24.0	*TCD1*	29.2		
YGR272C	13.2	*YCK1*	24.3	*TPM1*	29.2		

BUD19	13.3	*KNH1*	25.0	*YDR157W*	29.2
UGO1	13.3	*SHE4*	25.0	*YDR535C*	29.2
YBL065W	14.6	*SNF6*	25.0	*YNL097C-A*	29.2
SWI3	14.8	*YDL187C*	25.0	*YME1*	29.6
BRE4	15.2	*LRP1*	25.7	*NGG1*	30.3
YGR139W	15.6	*ACM1*	25.9	*POP2*	30.4
PMD1	15.8	*VCX1*	26.7	*ATP11*	30.8
YHL041W	15.8	*BUB1*	26.8	*RPL37B*	31.0
ERG28	16.7	*CCW12*	27.1	*HFI1*	31.0
SLX5	16.7	*HAM1*	27.1	*YML013C-A*	31.1

Table 3. Validated hyper-recombination genes from the patch assay and pinning assay screens.

Gene name	Description	Human orthologue(s)
HTA2	Histone H2A	H2A
NUP170	Subunit of inner ring of nuclear pore complex	NUP155
CSM1	Nucleolar protein that mediates homolog segregation during meiosis I	
YDL162C	Dubious open reading frame; overlaps the CDC9 promoter	LIG1
MSH6	Protein required for mismatch repair in mitosis and meiosis	MSH6
CHL4	Outer kinetochore protein required for chromosome stability	CENPN
RNH202	Ribonuclease H2 subunit	RNASEH2B
RAD4	Protein that recognizes and binds damaged DNA during NER	XPC
YER188W	Putative protein of unknown function	
DST1	General transcription elongation factor TFIIS	TCEA1, TCEA2, TCEA3
RAD6	Ubiquitin-conjugating enzyme	UBE2A, UBE2B
RRM3	DNA helicase involved in rDNA replication and Ty1 transposition	PIF1
THP2	Subunit of the THO and TREX complexes	
SKN7	Nuclear response regulator and transcription factor	HSF1, HSF2, HSF4, HSF5
HYR1	Thiol peroxidase	GPX1, GPX2, GPX3, GPX4, GPX5, GPX6, GPX7
RAD27	5' to 3' exonuclease, 5' flap endonuclease	FEN1
APN1	Major apurinic/apyrimidinic endonuclease	APE1

RNH203	Ribonuclease H2 subunit	RNASEH2C
TOP3	DNA Topoisomerase III	TOP3A
YLR235C	Dubious open reading frame; overlaps the TOP3 gene	TOP3A
YAP1	Basic leucine zipper transcription factor	
TSA1	Thioredoxin peroxidase	PRDX1, PRDX2, PRDX3, PRDX4
CSM3	Replication fork associated factor	TIPIN
MLH1	Protein required for mismatch repair in mitosis and meiosis	MLH1
SGS1	RecQ family nucleolar DNA helicase	BLM
ABZ2	Aminodeoxychorismate lyase (4-amino-4-deoxychorismate lyase)	
RNH201	Ribonuclease H2 catalytic subunit	RNASEH2A
PMS1	ATP-binding protein required for mismatch repair	PMS1
MGS1	Protein with DNA-dependent ATPase and ssDNA annealing activities	WRNIP1
TOF1	Subunit of a replication-pausing checkpoint complex	TIMELESS
MSH2	Protein that binds to DNA mismatches	MSH2
DFG16	Probable multiple transmembrane protein	
ELG1	Subunit of an alternative replication factor C complex	ATAD5
RMI1	Subunit of the RecQ (Sgs1) - Topo III (Top3) complex	RMI1
VMA11	Vacuolar ATPase V0 domain subunit c'	ATP6VOC